3I/ATLAS - portret międzygwiazdowej komety

Piotr Guzik

Jagiellonian University, Kraków, Poland

3 grudnia 2025

Introduction: comets and asteroids

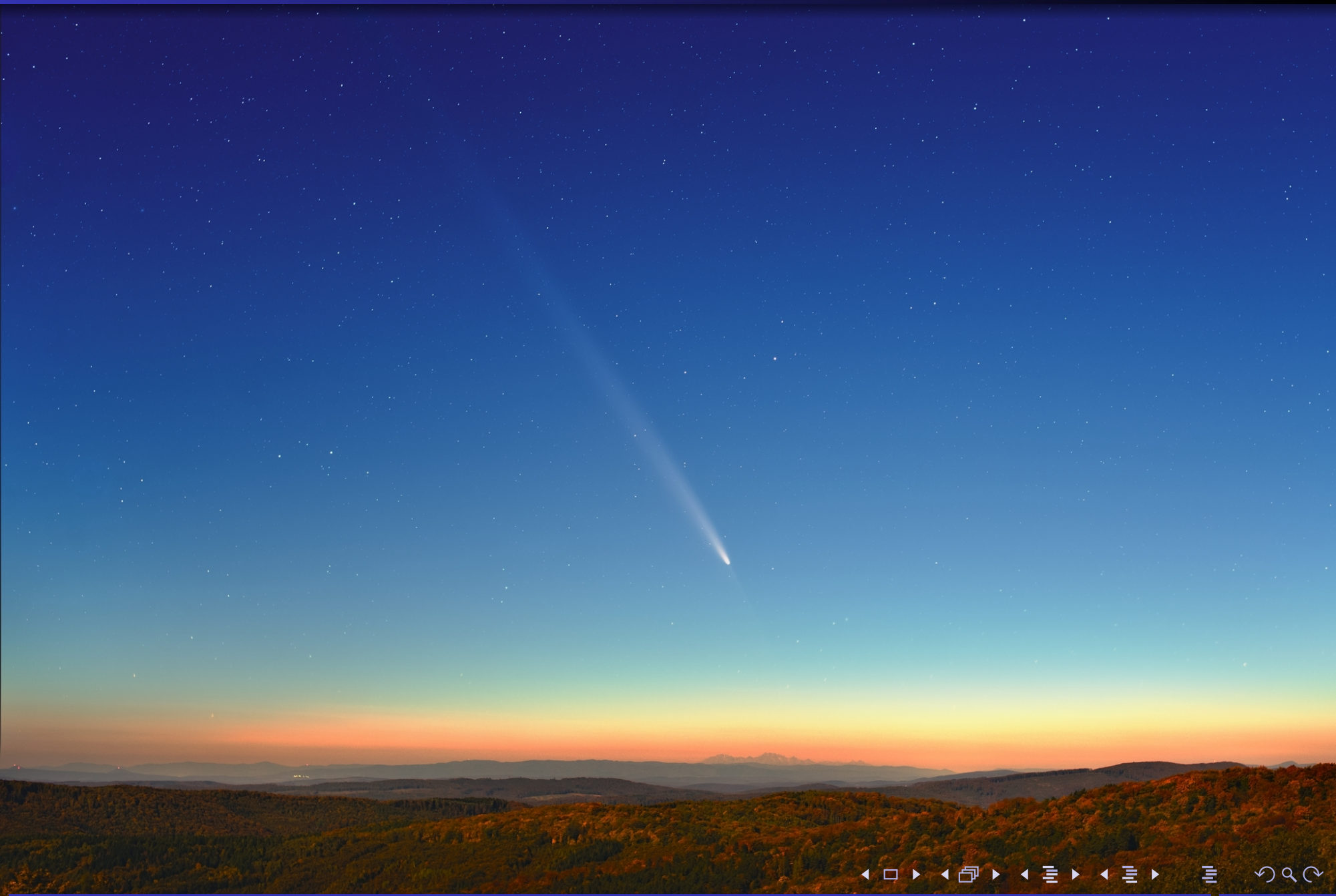

Introduction: interstellar minor bodies - early expectations

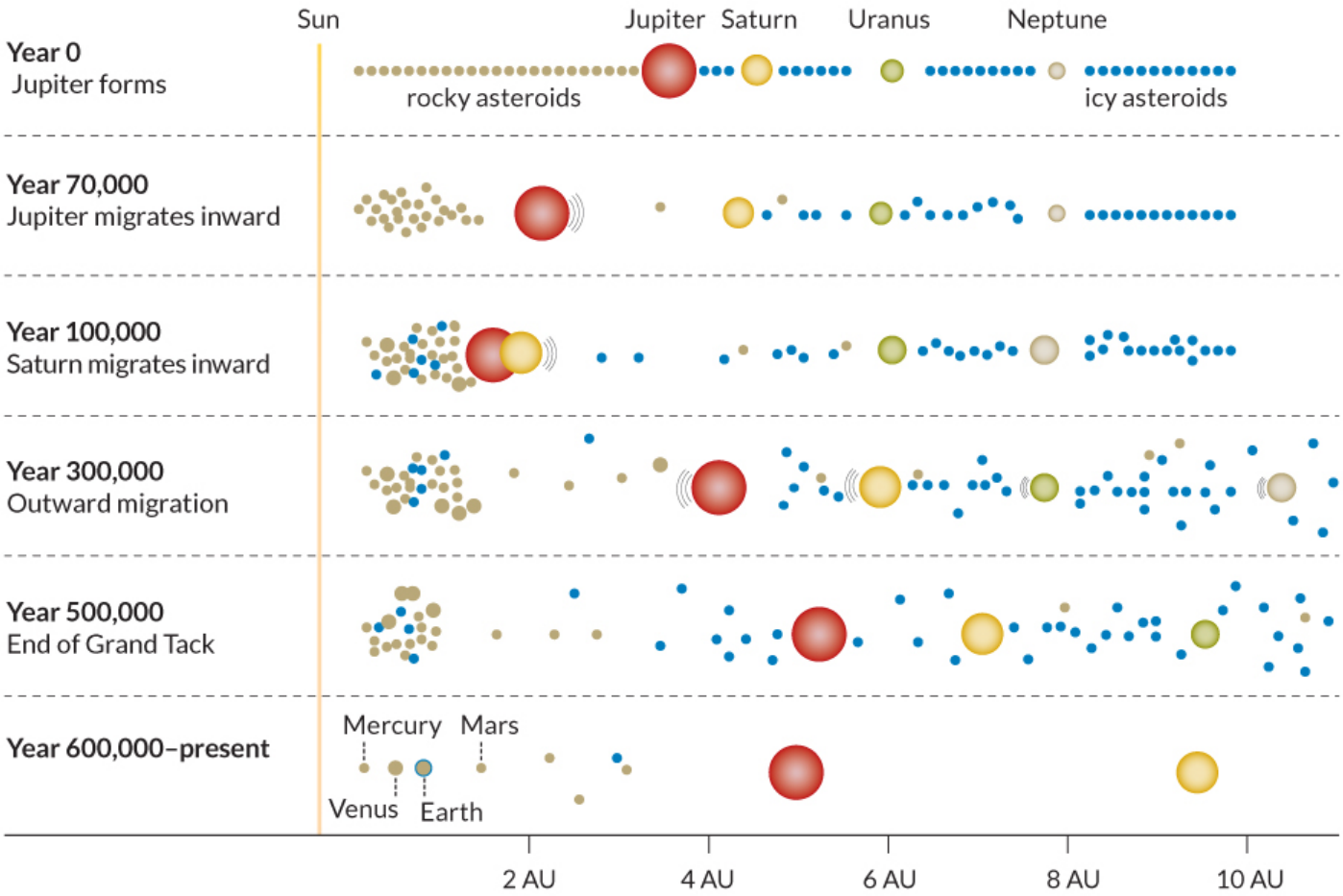

Giant planet formation and migration. *source: https://www-n.oca.eu/*

Introduction: interstellar minor bodies - discoveries

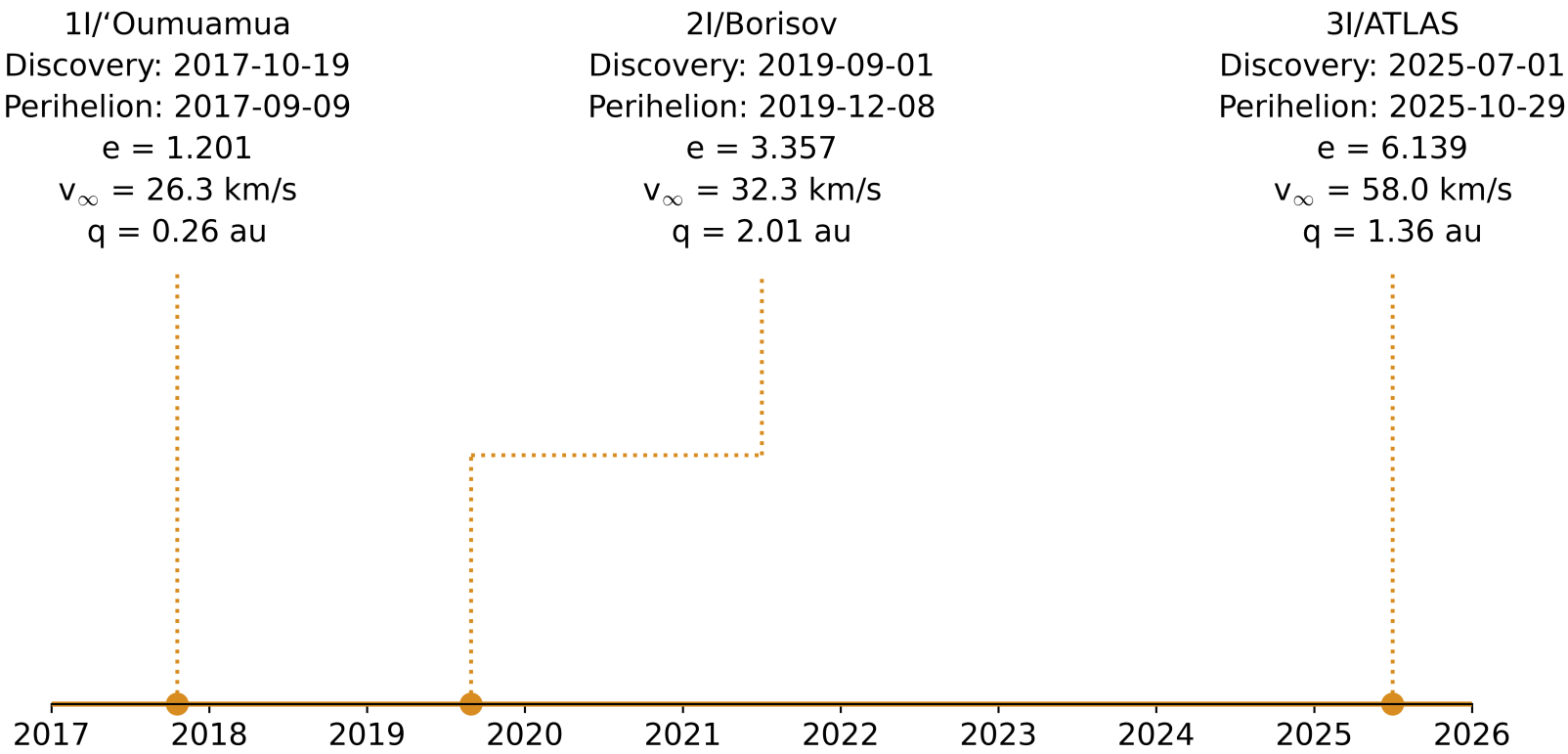

Timeline of interstellar visitors and their hyperbolic orbits.

Introduction: 1I/'Oumuamua and 2I/Borisov

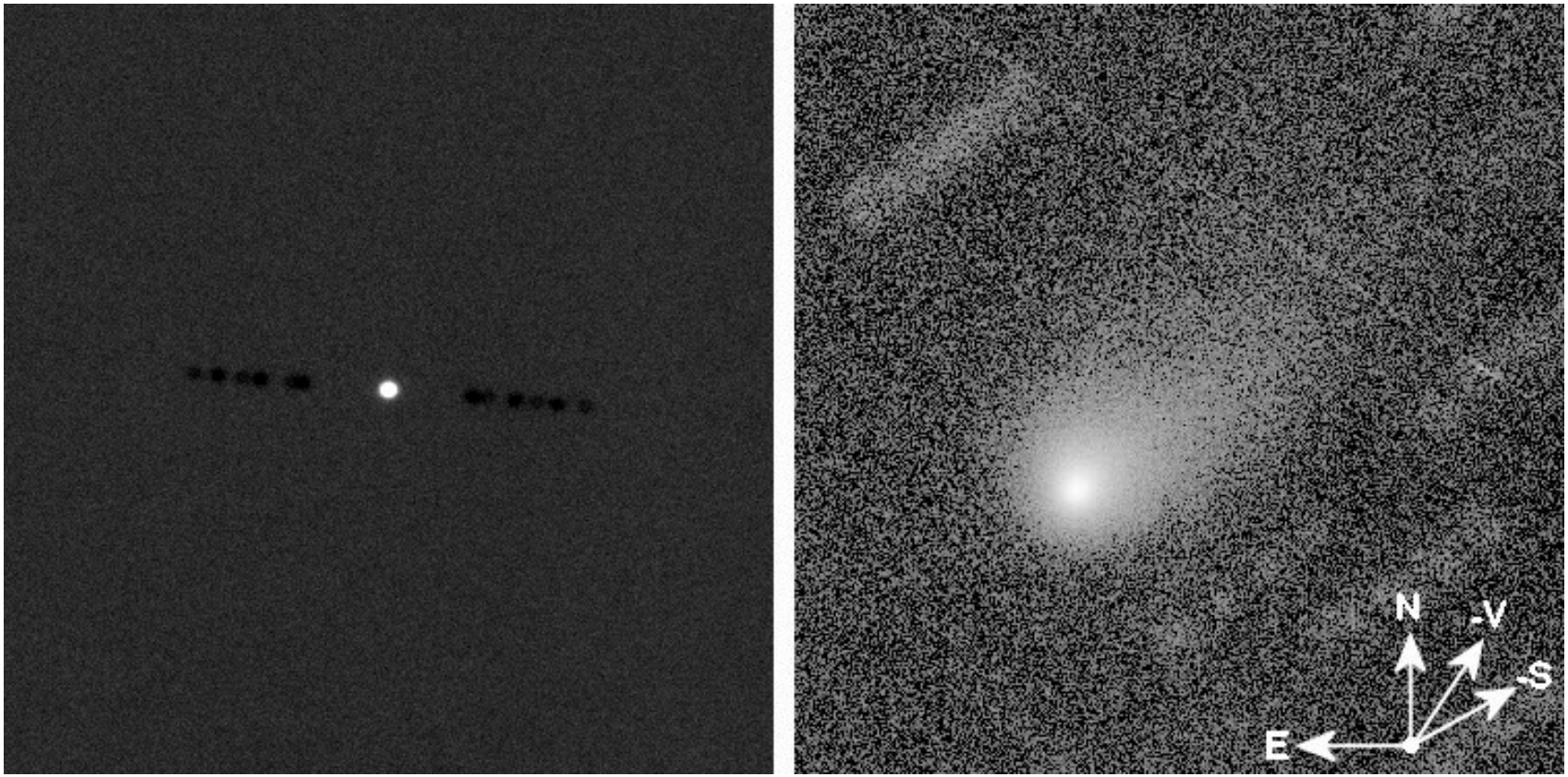

1I/'Oumuamua (left) and 2I/Borisov (right) observed with the Gemini North telescope. From Drahus et al. (2018, Nat. Astron. 2, 407) and Guzik et al. (2020, Nat. Astron. 4, 53), respectively.

3I/ATLAS: discovery

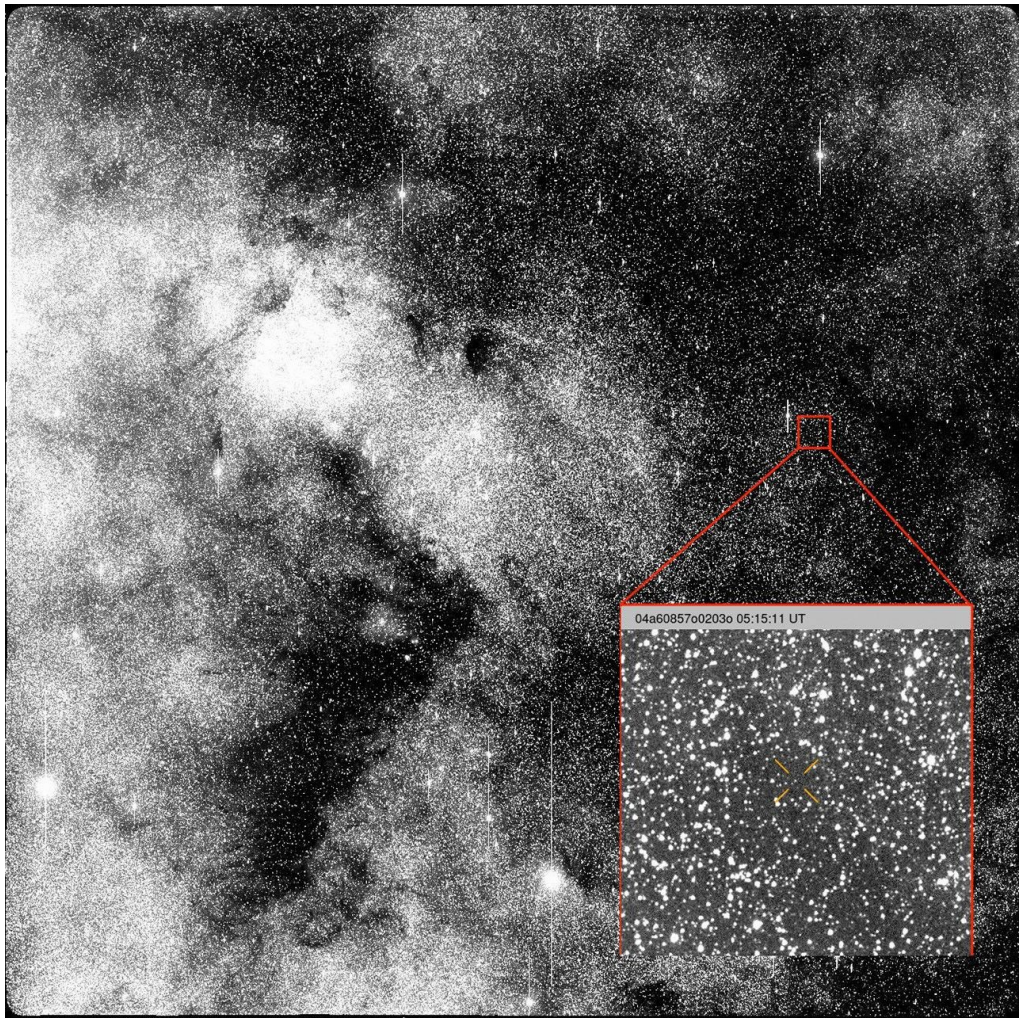

The discovery image of 3I/ATLAS taken on 1 July 2025.
Image Credit: ATLAS/University of Hawaii/NASA

3I/ATLAS: orbit

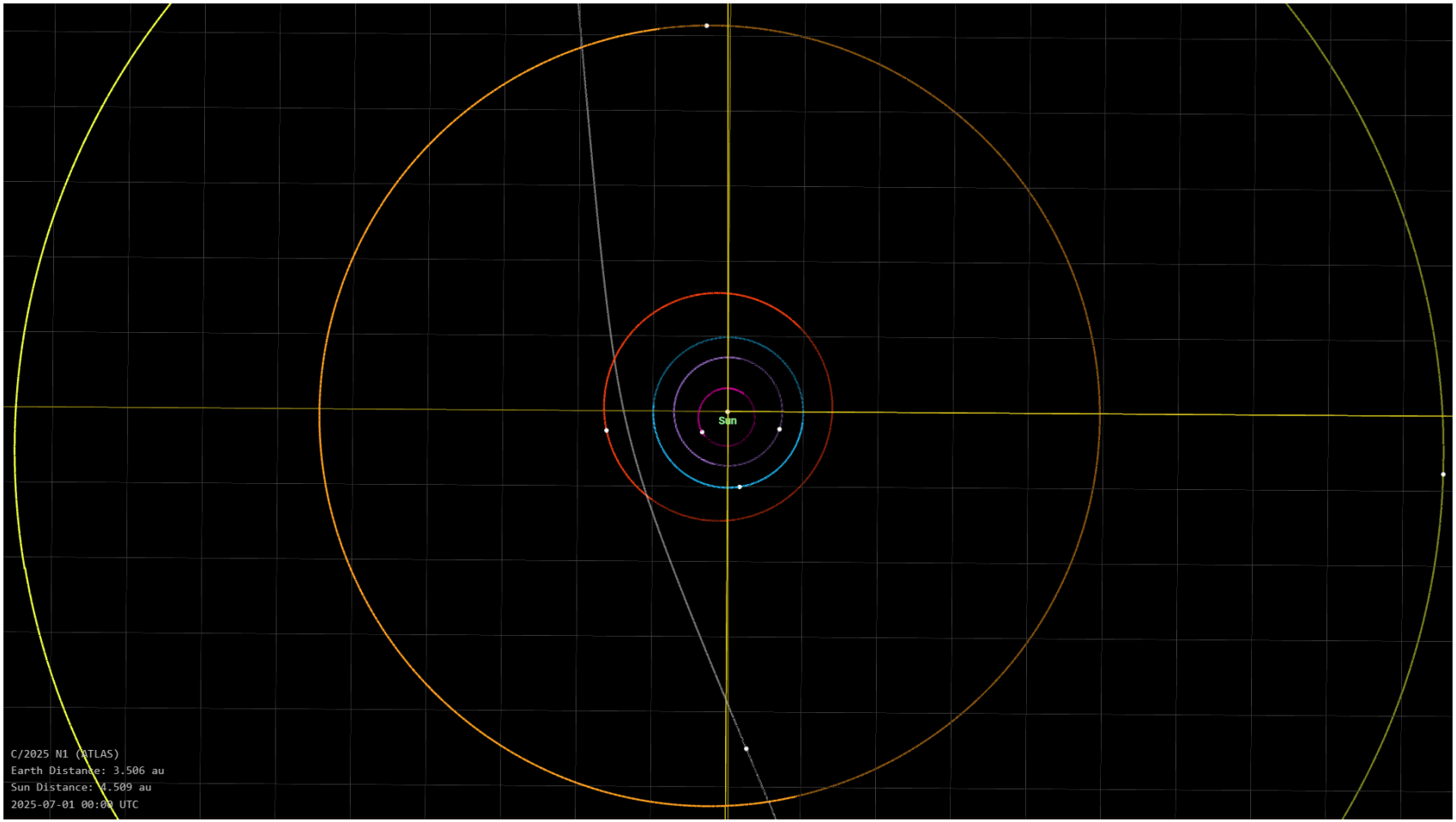

Position at the time of discovery. *source: NASA/JPL-Caltech*

3I/ATLAS: orbit

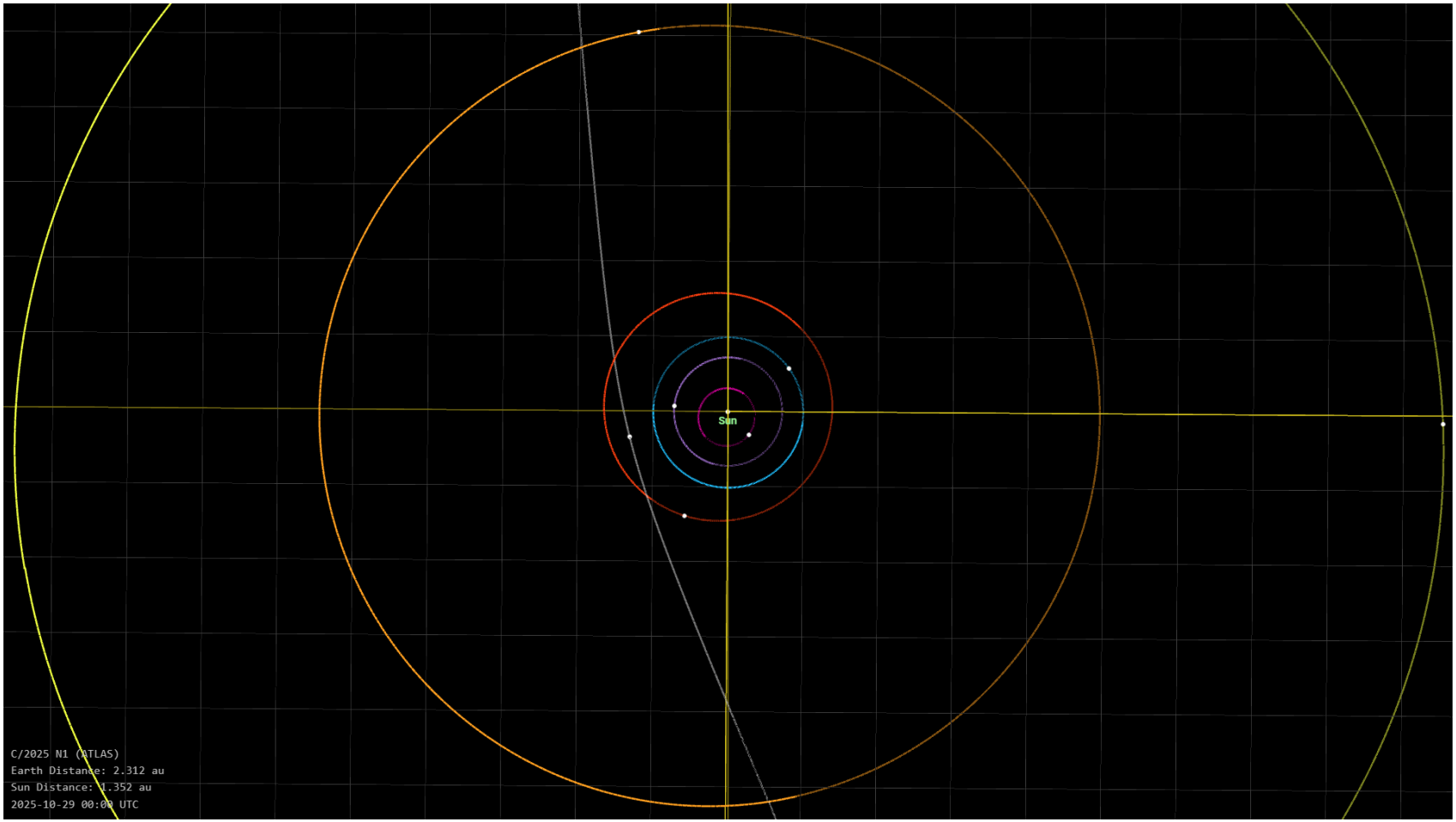

Position at the time of perihelion passage. *source: NASA/JPL-Caltech*

3I/ATLAS: orbit

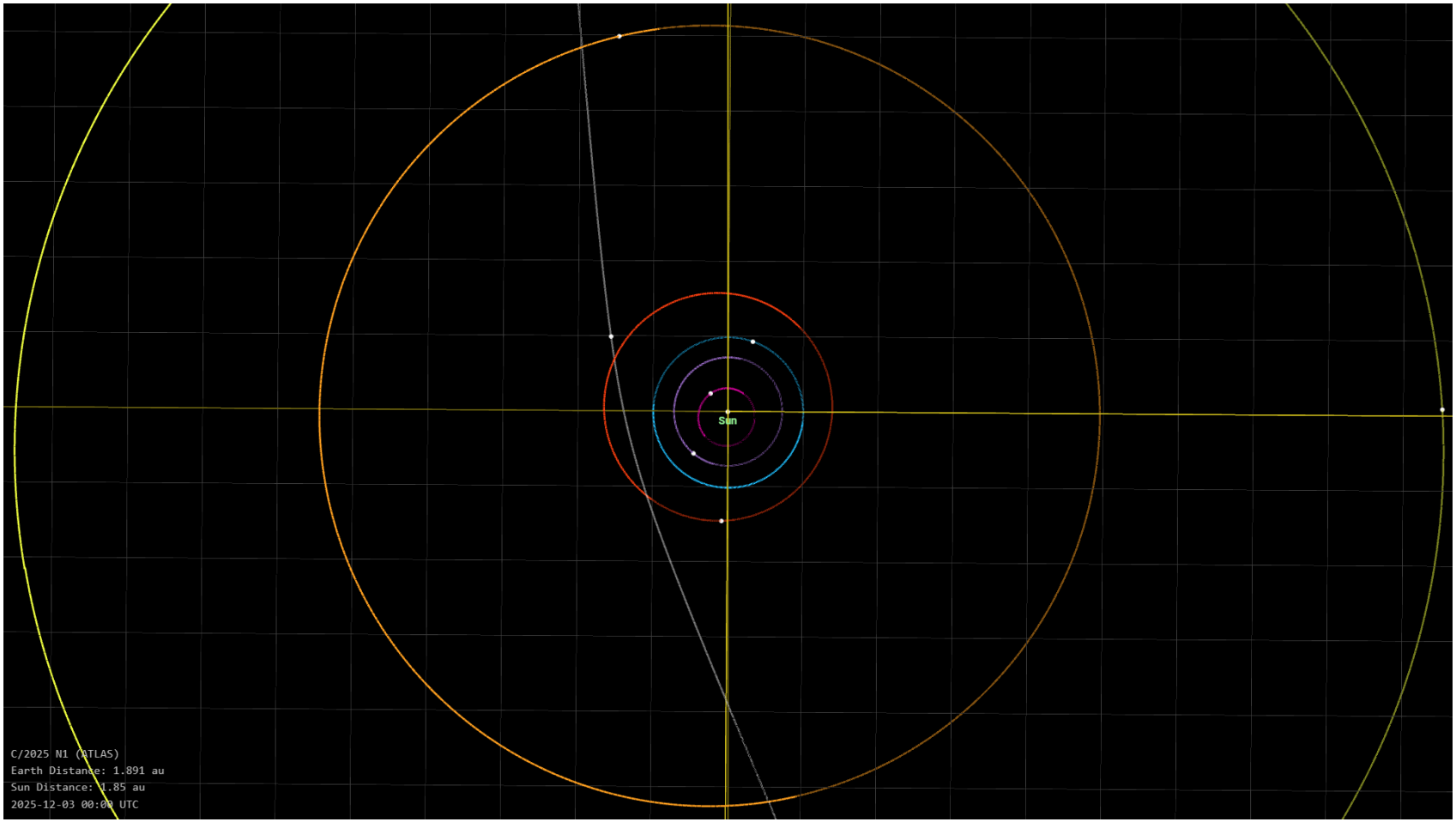

Position right now (3 Dec 2025). *source: NASA/JPL-Caltech*

3I/ATLAS: orbit

- Perihelion distance: $q \simeq 1.36\ \mathrm{au}$ (2025-10-29).
- Eccentricity: $e \simeq 6.1$ (strongly hyperbolic).
- Hyperbolic excess: $v_\infty \simeq 58\ \mathrm{km\,s^{-1}}$.
- Inclination: $i \simeq 175^\circ$ (retrograde, nearly ecliptic).

- Closest to Mars: $\Delta_{\mathrm{Mars}} \approx 0.19$ au.
- Closest to Venus: $\Delta_{\mathrm{Venus}} \approx 0.65$ au.
- Closest to Earth: $\Delta_{\oplus} \approx 1.8$ au.
- Passage by Jupiter: $\Delta_{\mathrm{Jup}} \approx 0.36$ au.

3I/ATLAS: Galactic kinematic context

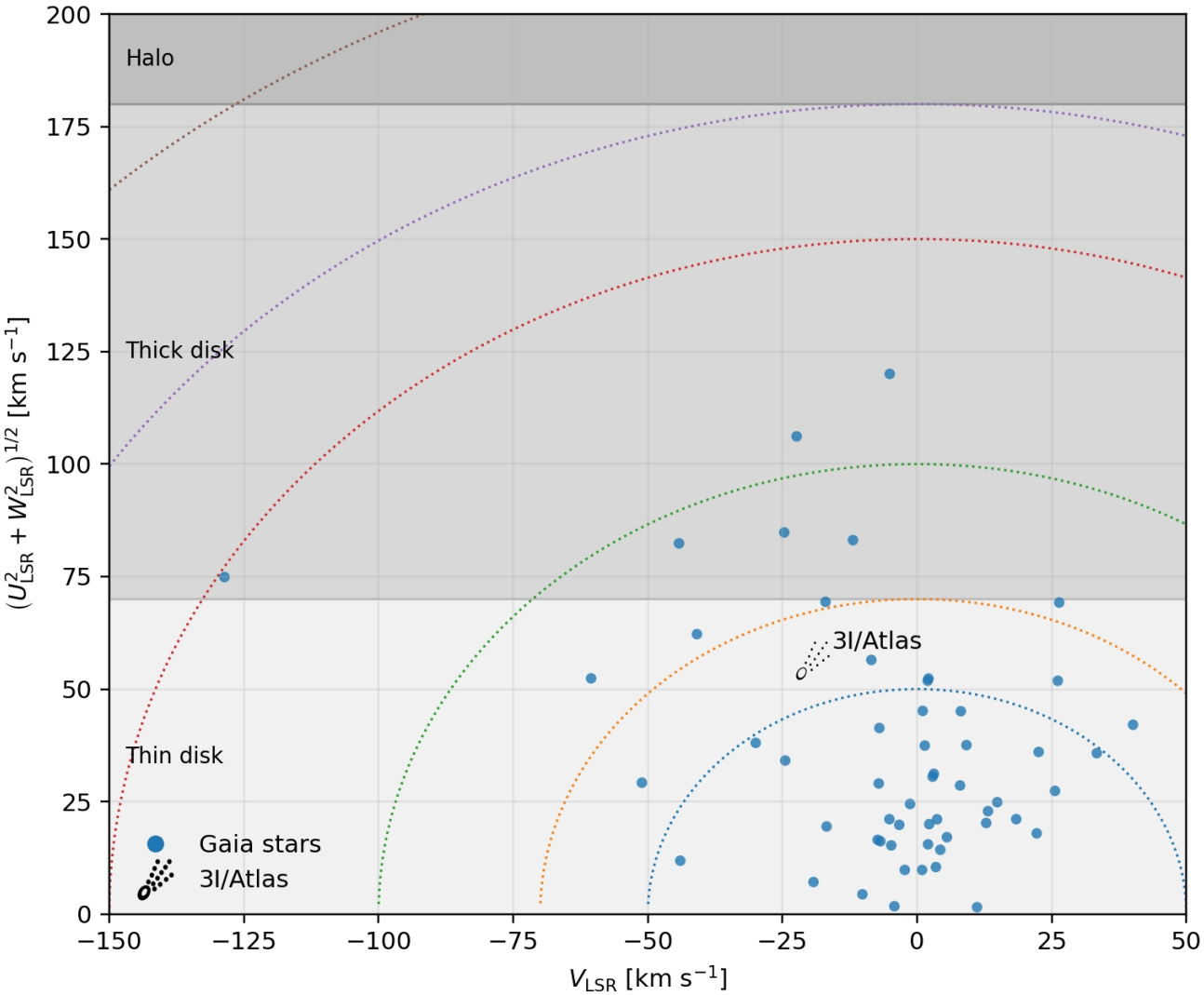

Toomre diagram for 3I/ATLAS (Perez-Couto et al. 2025).

3I/ATLAS: Galactic trajectory

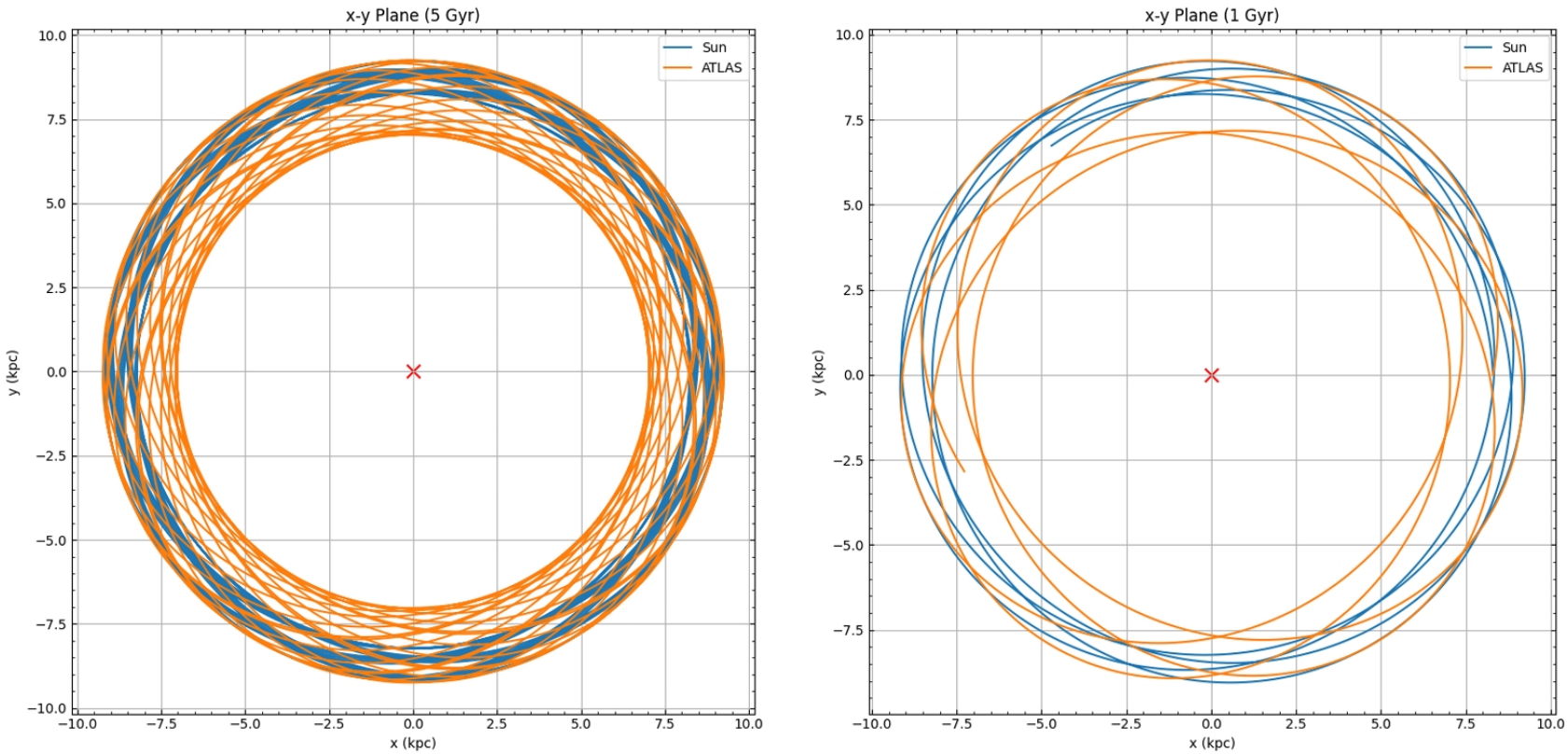

Trajectories of 3I/ATLAS and the Sun in the x-y plane of Milky Way, integrated 5 Gyr (left) and 1 Gyr (right) backwards. (Kakharov & Loeb 2025).

3I/ATLAS: Galactic trajectory

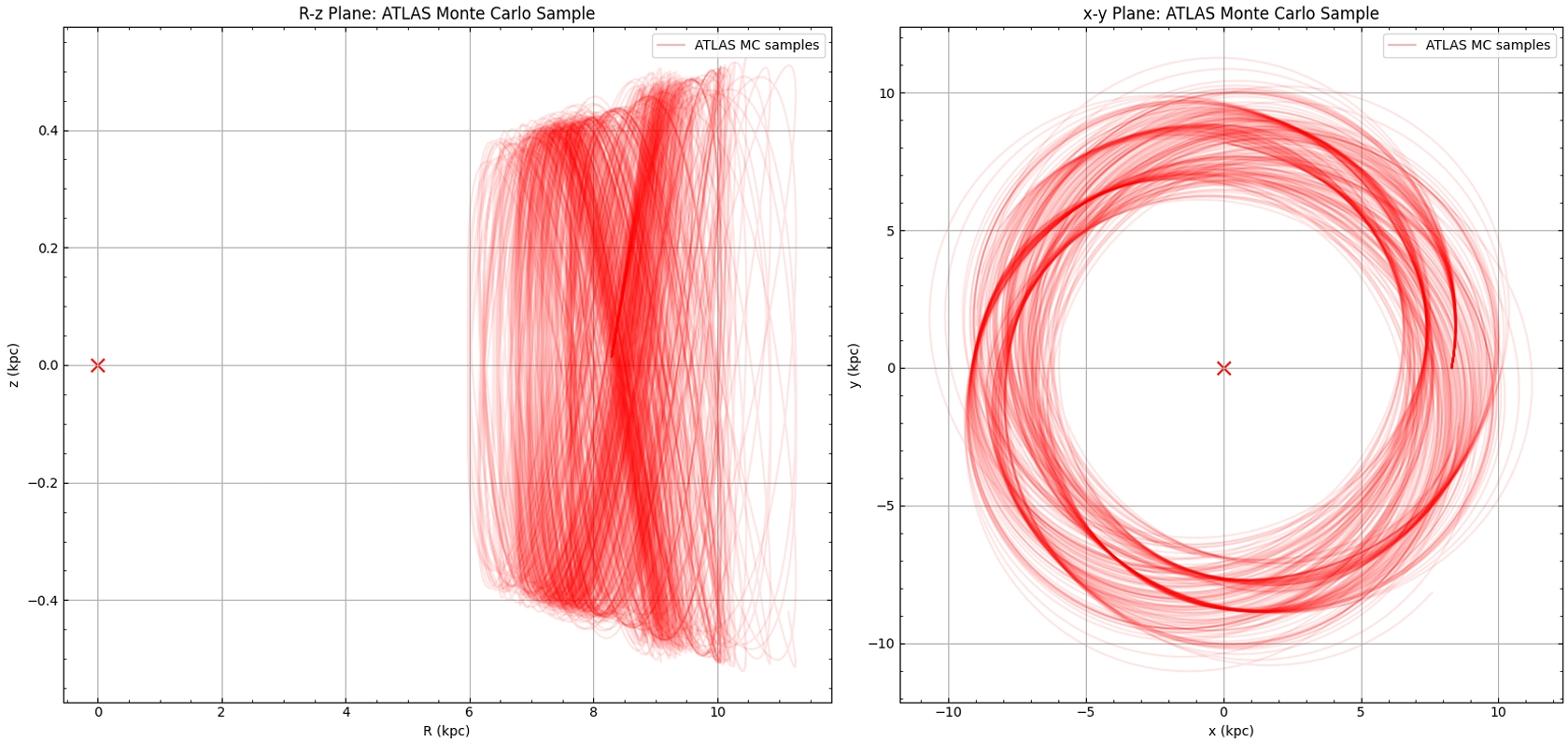

Ensemble of backward integrated Monte Carlo trajectories of 3I/ATLAS (Kakharov & Loeb 2025).

3I/ATLAS: ZTF - prediscovery images

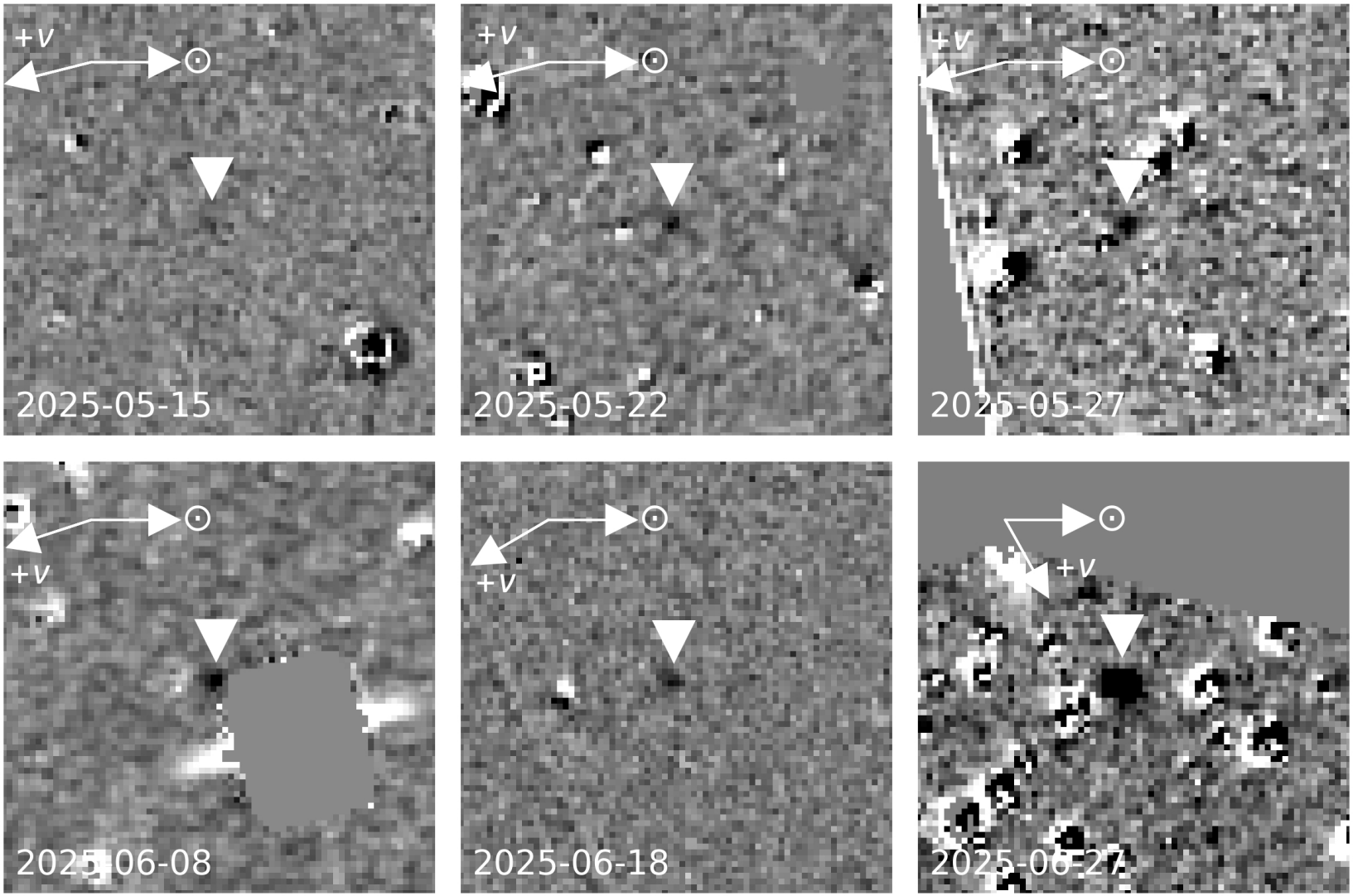

Pre-discovery images of 3I/ATLAS made by the Zwicky Transient Facility (ZTF) (adapted from Ye et al. 2025).

3I/ATLAS: ZTF - early activity

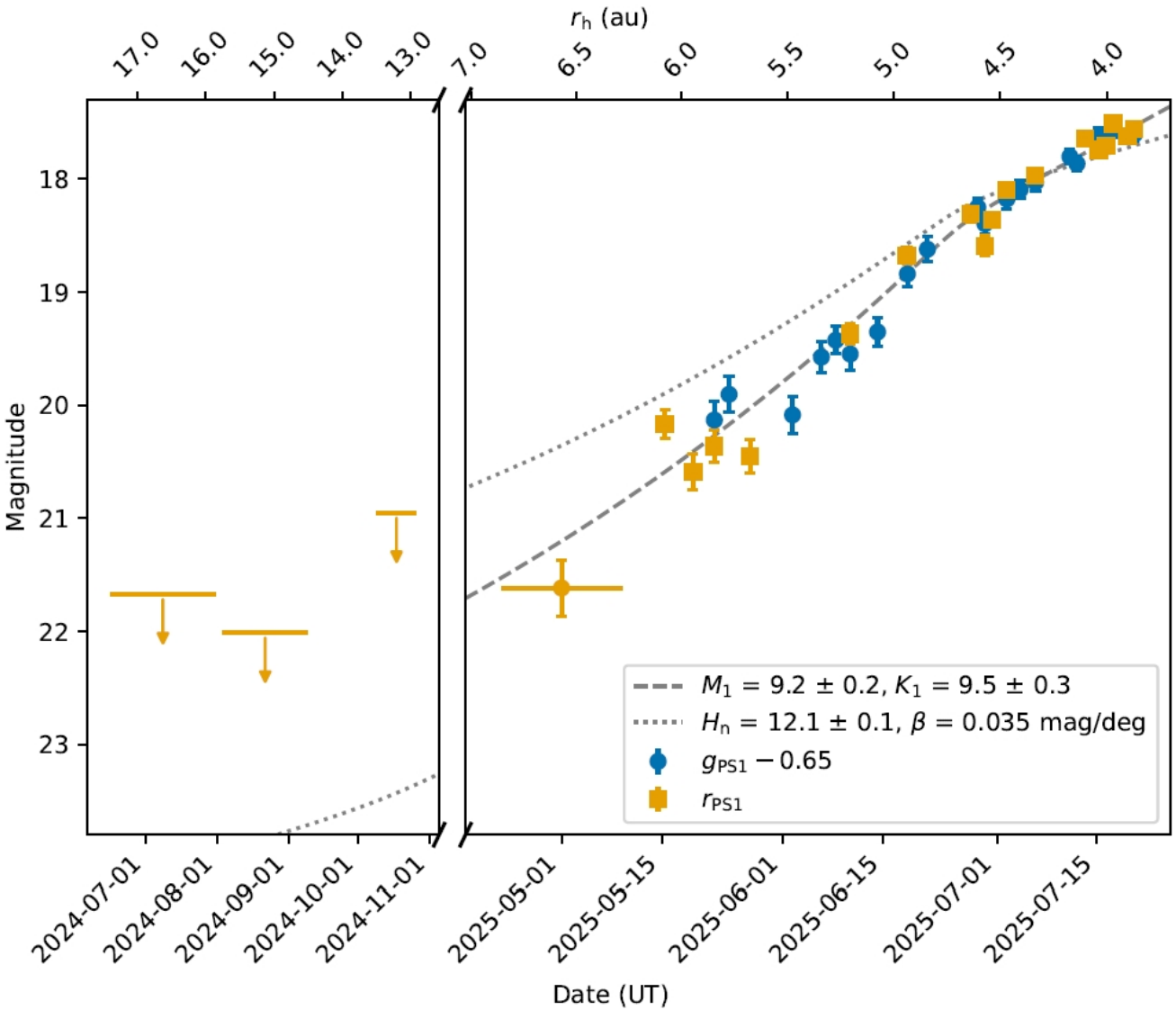

ZTF photometry indicating early onset of cometary activity (Ye et al. 2025).

3I/ATLAS: rotational lightcurve

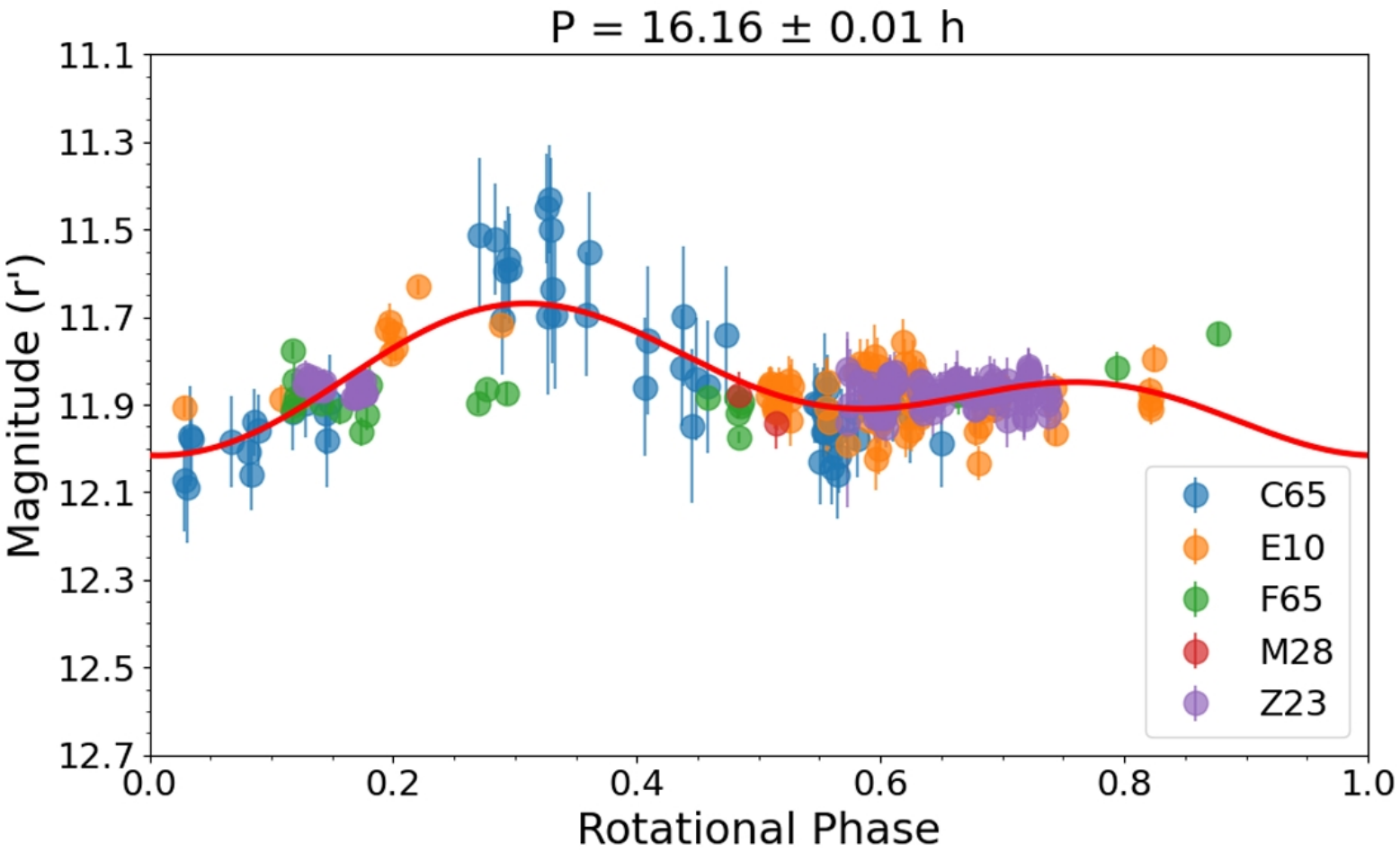

Rotational lightcurve obtained with multiple ground-based telescopes (Santana-Ros et al. 2025).

3I/ATLAS: early spectrum

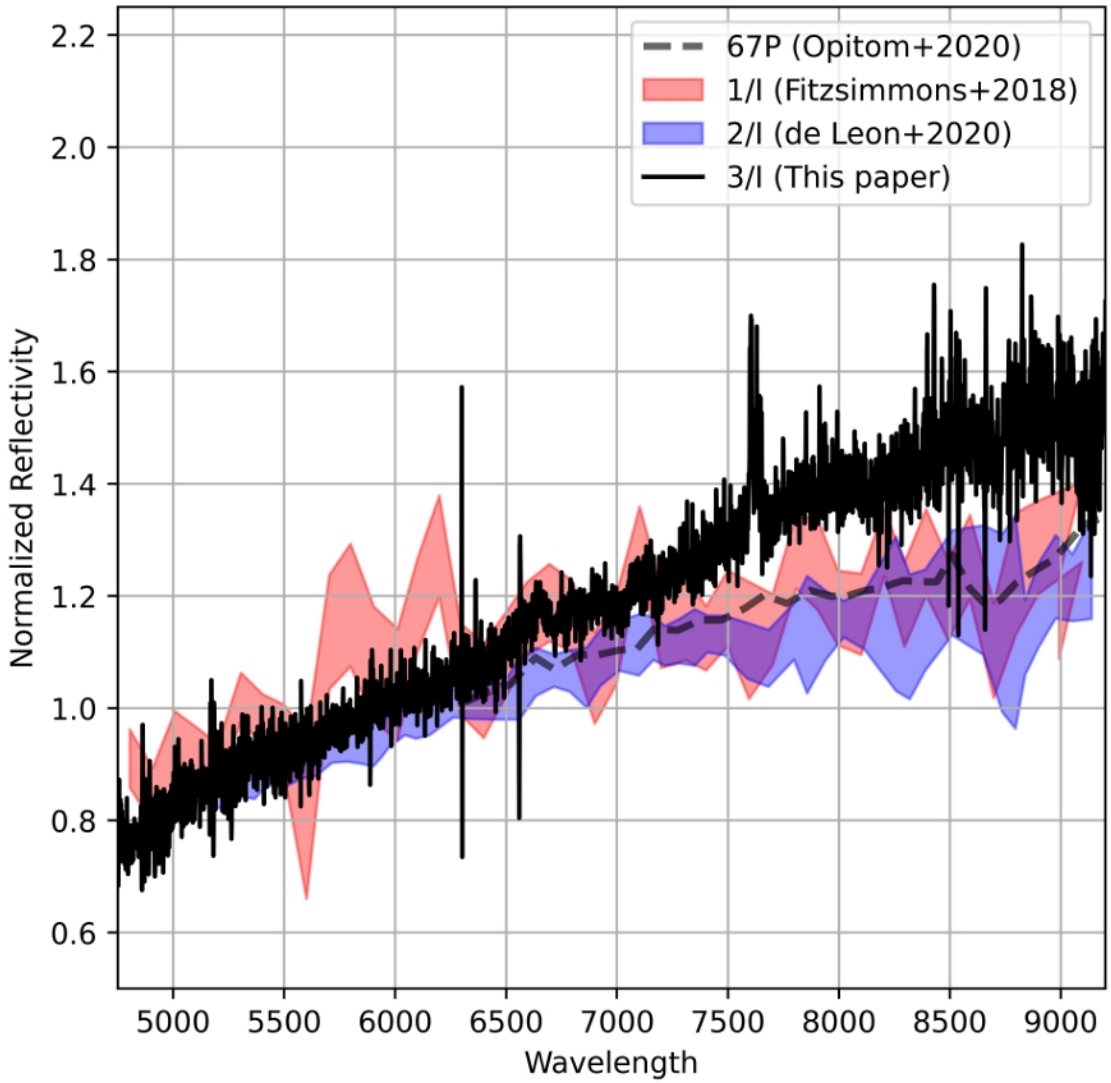

Early optical reflectance spectrum of 3I/ATLAS – red, nearly featureless continuum (Opitom et al. 2025)

3I/ATLAS: HST observations

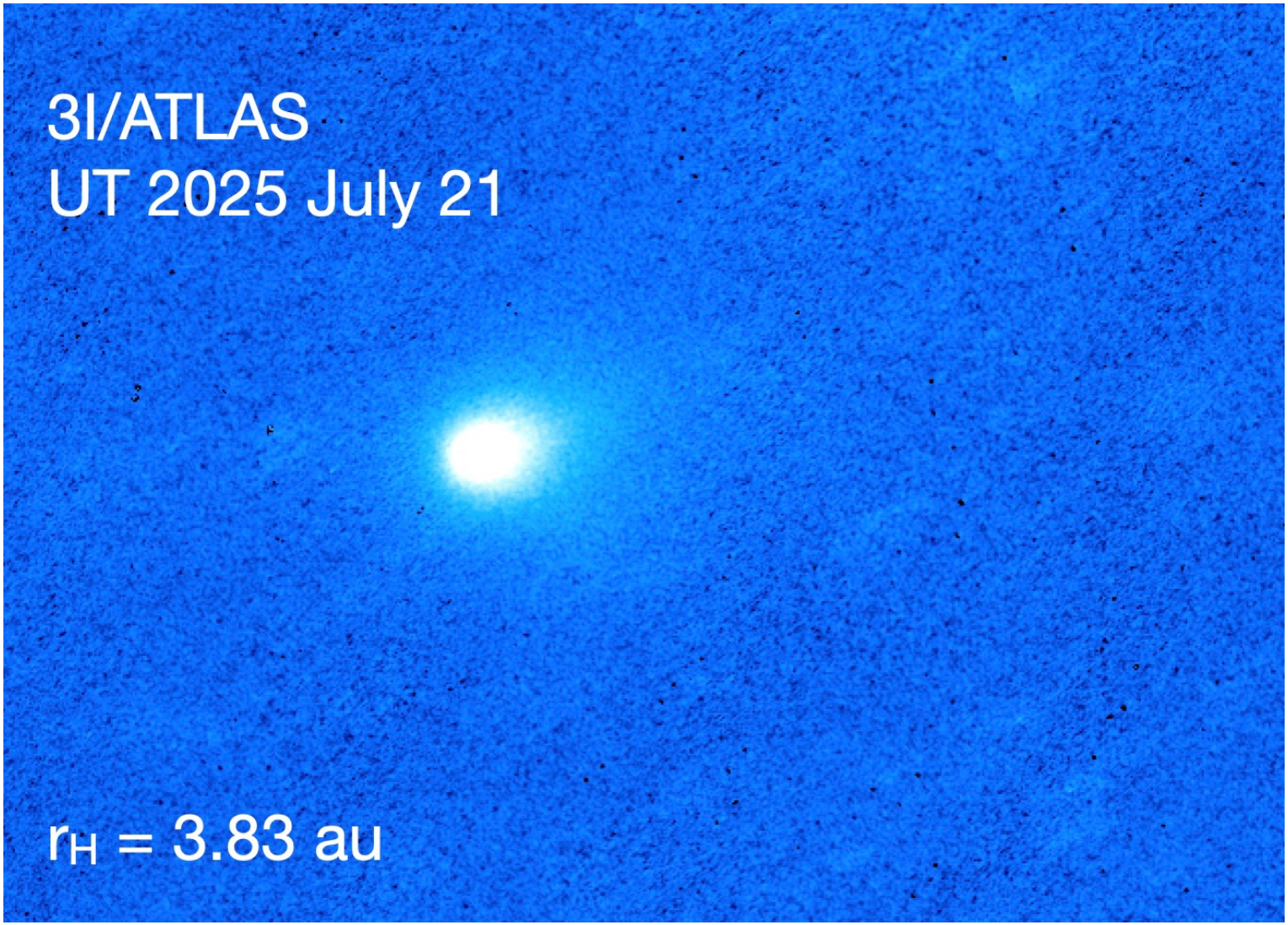

Early image of 3I/ATLAS obtained with the Hubble Space Telescope (Jewitt et al. 2025), showing a prominent sunward jet.

3I/ATLAS: nucleus size and rotation

- Nucleus diameter
  - Early photometric estimates: $r_{\rm n} \lesssim 10$ km
  - HST constraints (Jewitt et al. 2025):

$$0.16 \lesssim r_{\rm n} \lesssim 2.8 \ {\rm km}$$

- Rotational period
  - $P_{\rm rot} = 16.16 \pm 0.01$ h (multi-site ground-based photometry; Santana-Ros et al. 2025).
  - $P_{\rm rot} \approx 16.8$ h (GTC + TTT photometry; de la Fuente Marcos et al. 2025).
  - No robust period detected in the TESS precovery light curve (Feinstein et al. 2025).

3I/ATLAS: NOT - morphological development

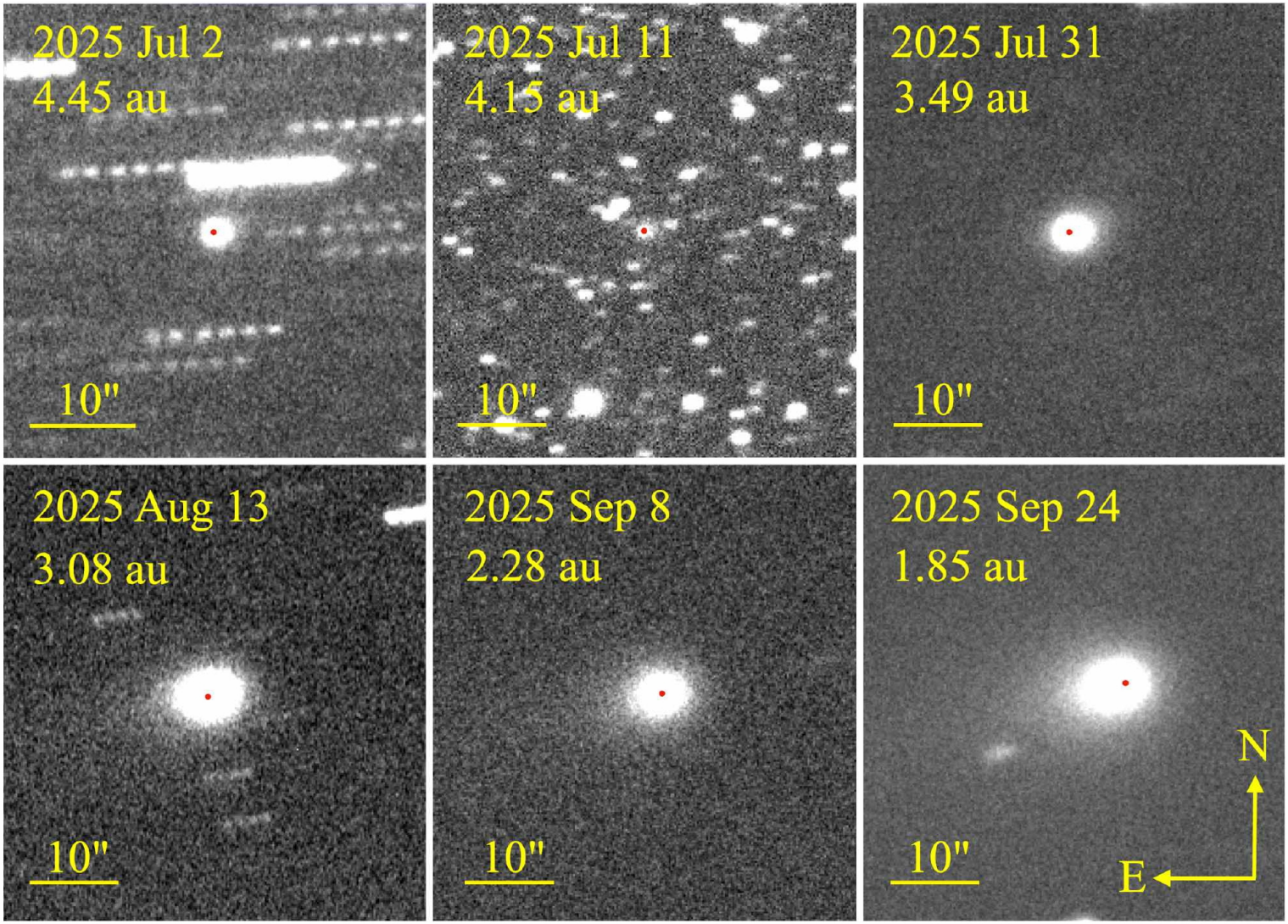

Pre-perihelion morphological development of 3I/ATLAS (Jewitt et al. 2025).

3I/ATLAS: JWST/NIRSpec integrated spectrum

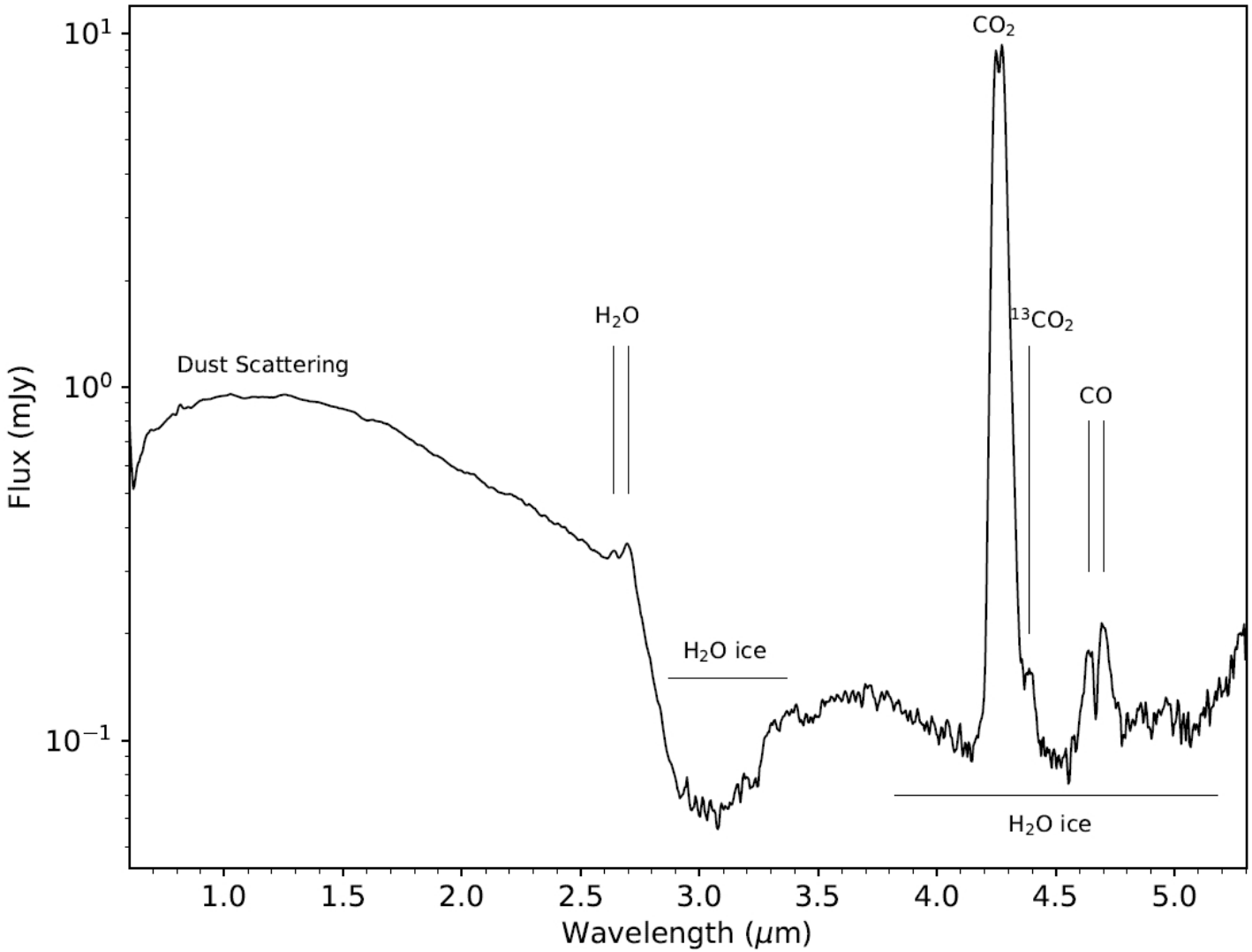

Spatially integrated JWST/NIRSpec prism spectrum of 3I/ATLAS at $r_{\rm H} = 3.32$ au (Cordiner et al. 2025).

3I/ATLAS: JWST coma structure (IFU maps)

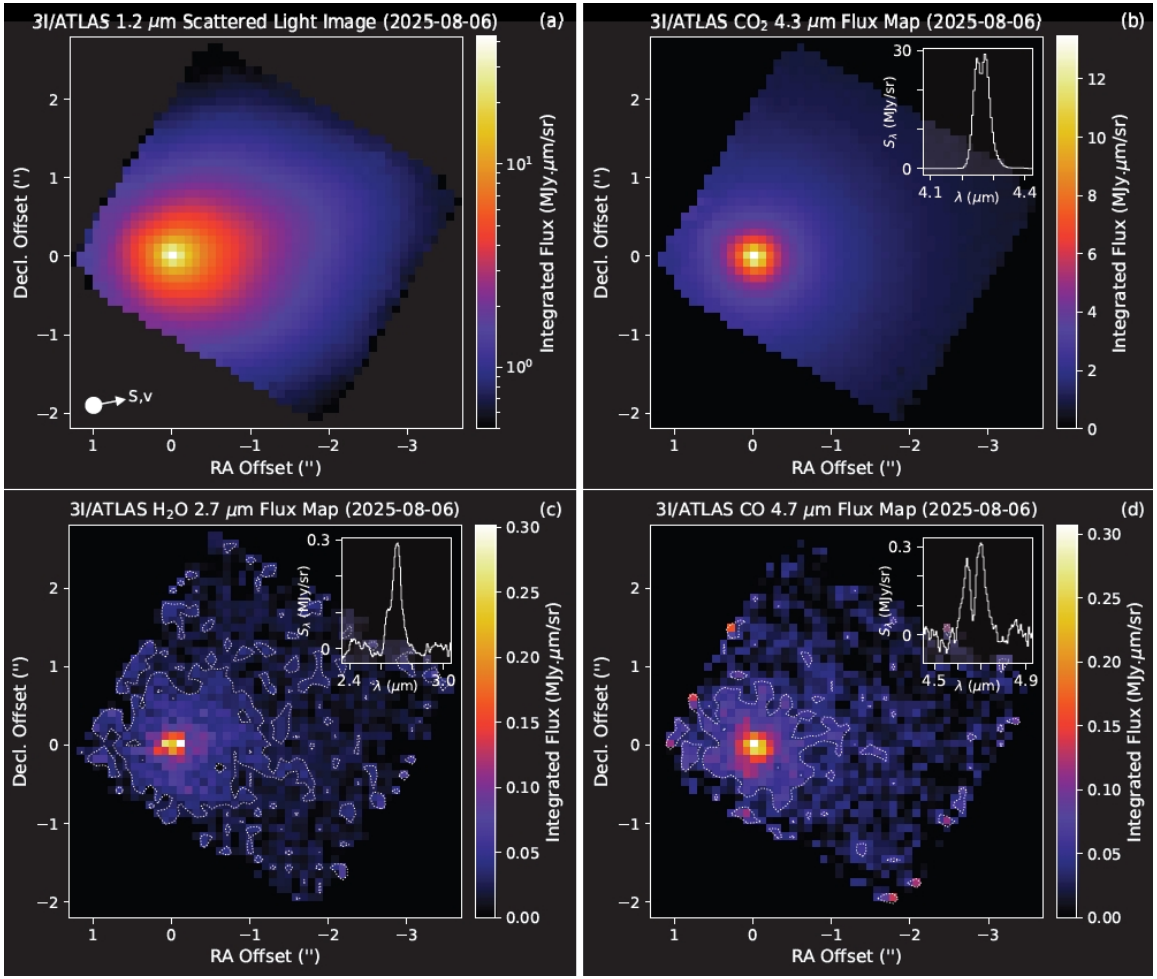

JWST/NIRSpec IFU flux maps of 3I/ATLAS: dust-scattered continuum, CO_2, H_2O and CO (Cordiner et al. 2025).

3I/ATLAS: volatile composition (overview)

- JWST/NIRSpec at $r_{\mathrm{H}} \simeq 3.3$ au: CO_2-dominated coma.
- Mixing ratios: $CO_2/H_2O \sim 7$–8, $CO/H_2O \sim 1$–2, OCS detected.
- Strong water-ice absorption bands, small icy grains in the coma.
- CO_2/H_2O far above Solar System comet trends.

3I/ATLAS: CO_2/H_2O vs Solar System comets

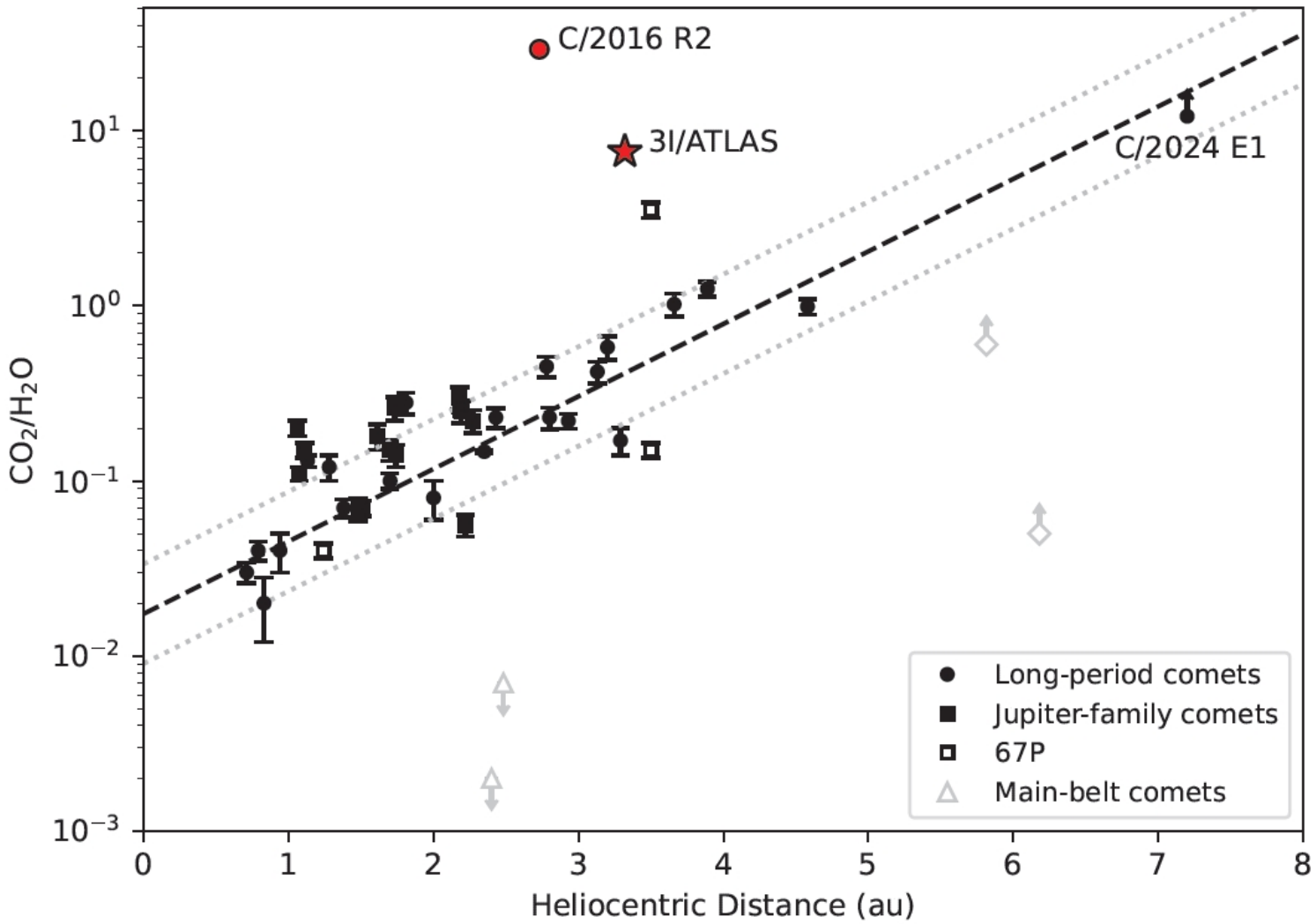

CO_2/H_2O mixing ratio for 3I/ATLAS compared to long-period and Jupiter-family comets (Cordiner et al. 2025).

3I/ATLAS: evidence for a cosmic-ray processed mantle

- Very high CO_2/H_2O and CO/H_2O.
- Extended CO_2 coma of small icy grains.
- Galactic cosmic rays convert CO-rich ices into CO_2 and organics in outer layers.
- Processed mantle depth $\sim$ 10–20 m after Gyr in interstellar space.

3I/ATLAS: schematic cross-section

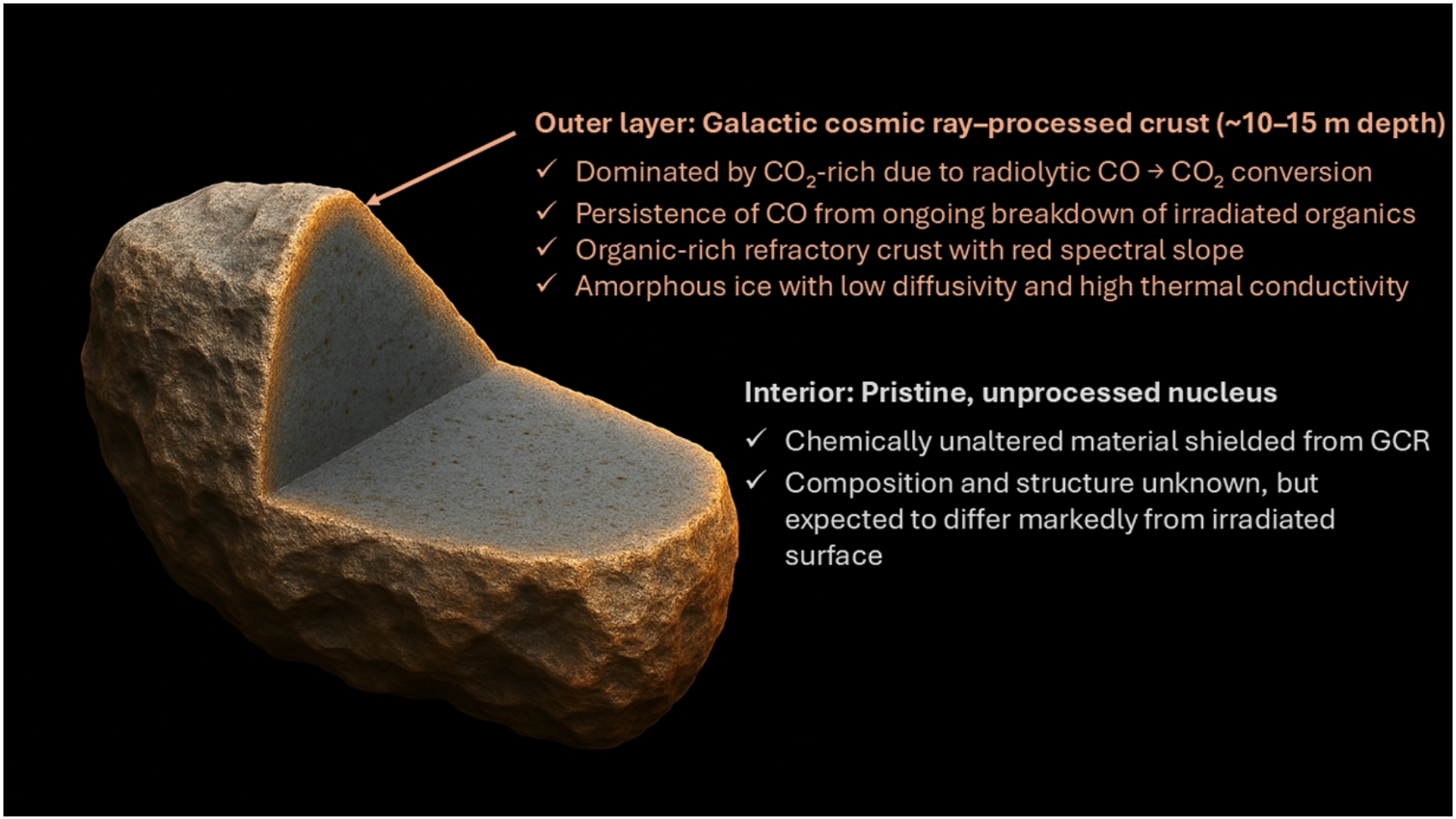

Schematic structure of 3I/ATLAS: a cosmic-ray processed, CO_2-rich outer mantle over a more pristine interior (Maggiolo et al. 2025).

3I/ATLAS: VLT spectra (Ni and CN)

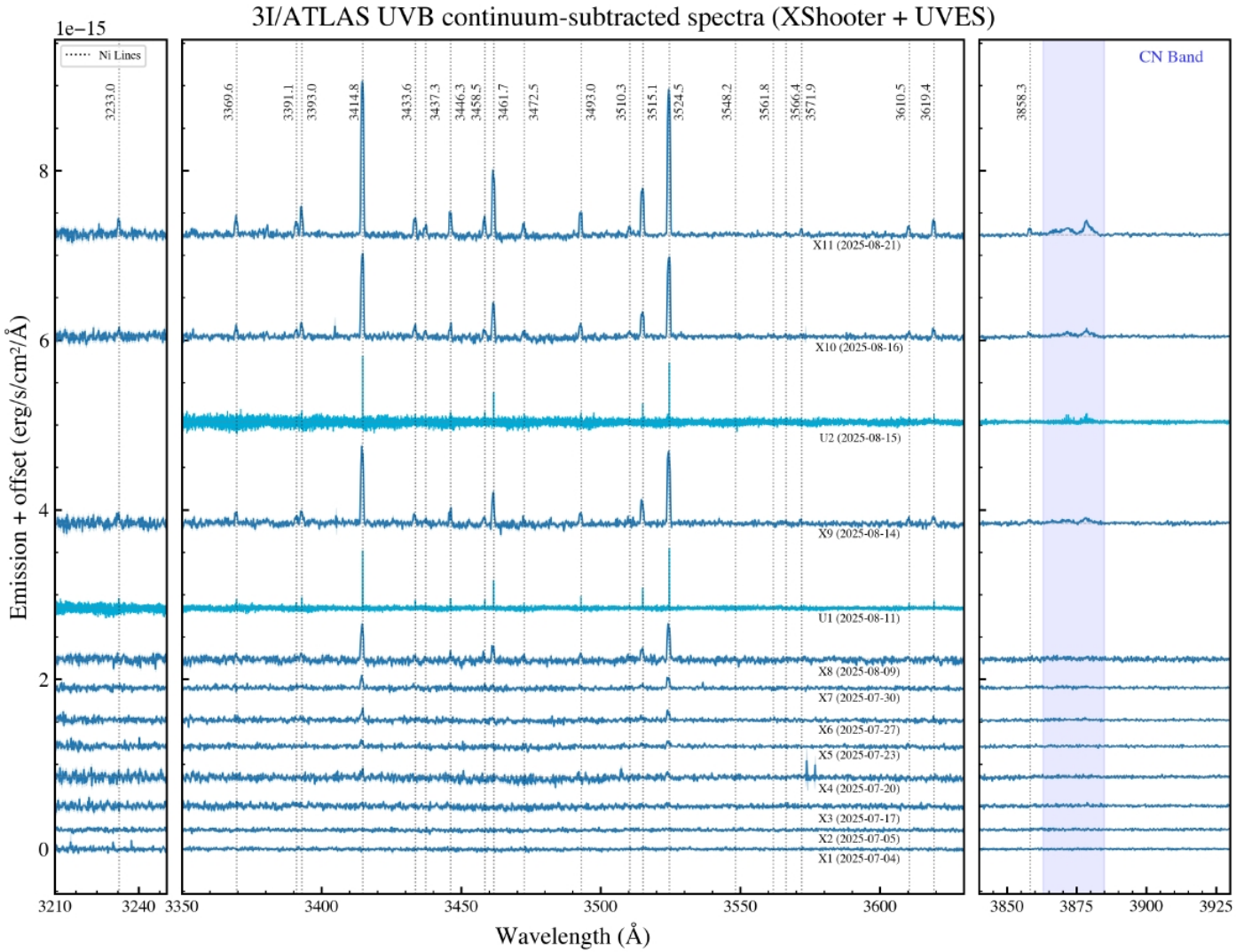

Evolution of Ni I and CN emission in VLT/UVES/X-shooter spectra of 3I/ATLAS from $r_{\mathrm{H}} \sim 4.4$ to 2.9 au (after Rahatgaonkar et al. 2025).

3I/ATLAS: VLT spectra - Ni production rates

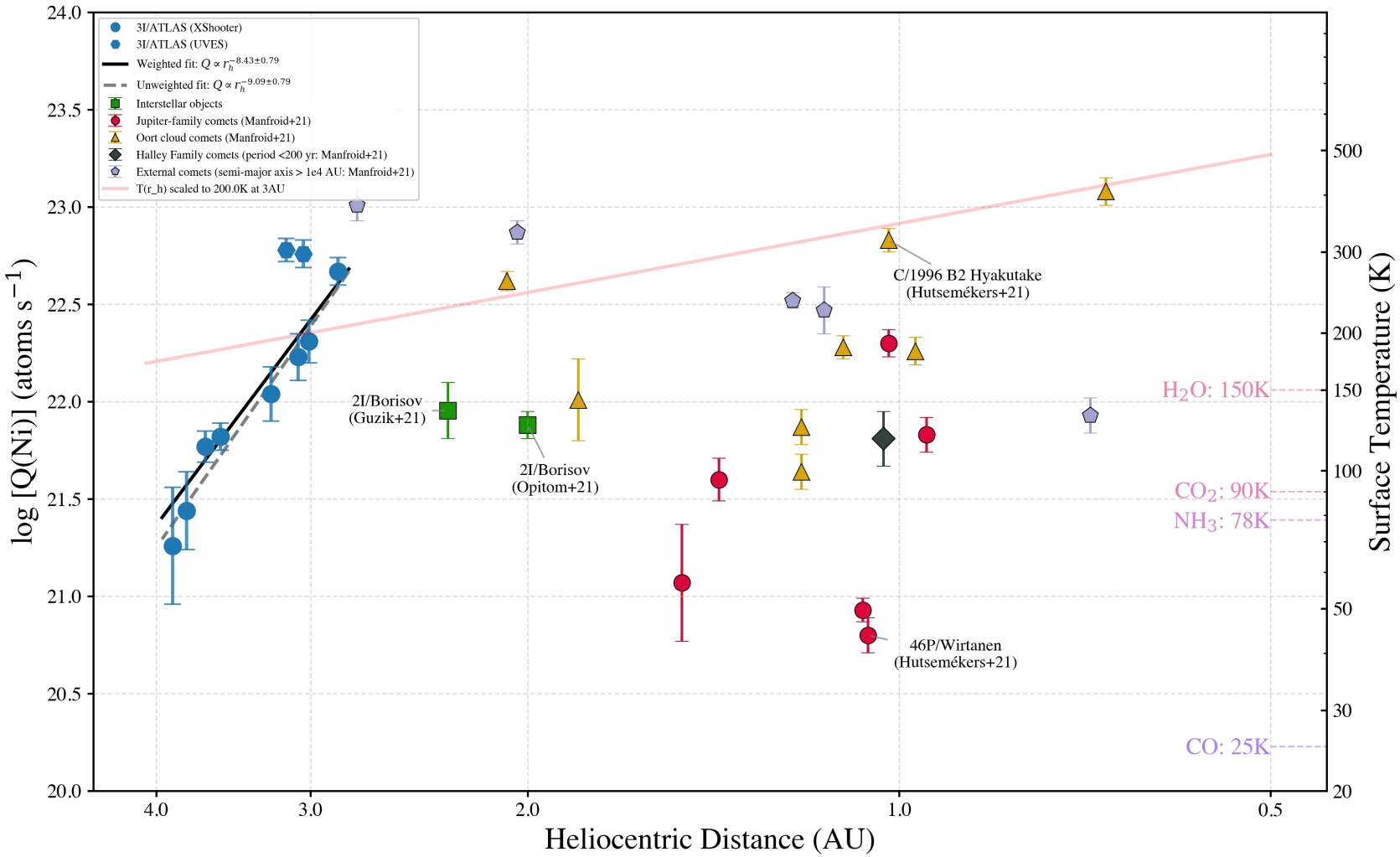

Ni production rates – comparison with Solar System comets and 2I/Borisov (Rahatgaonkar et al. 2025).

3I/ATLAS: VLT spectra - CN production rates

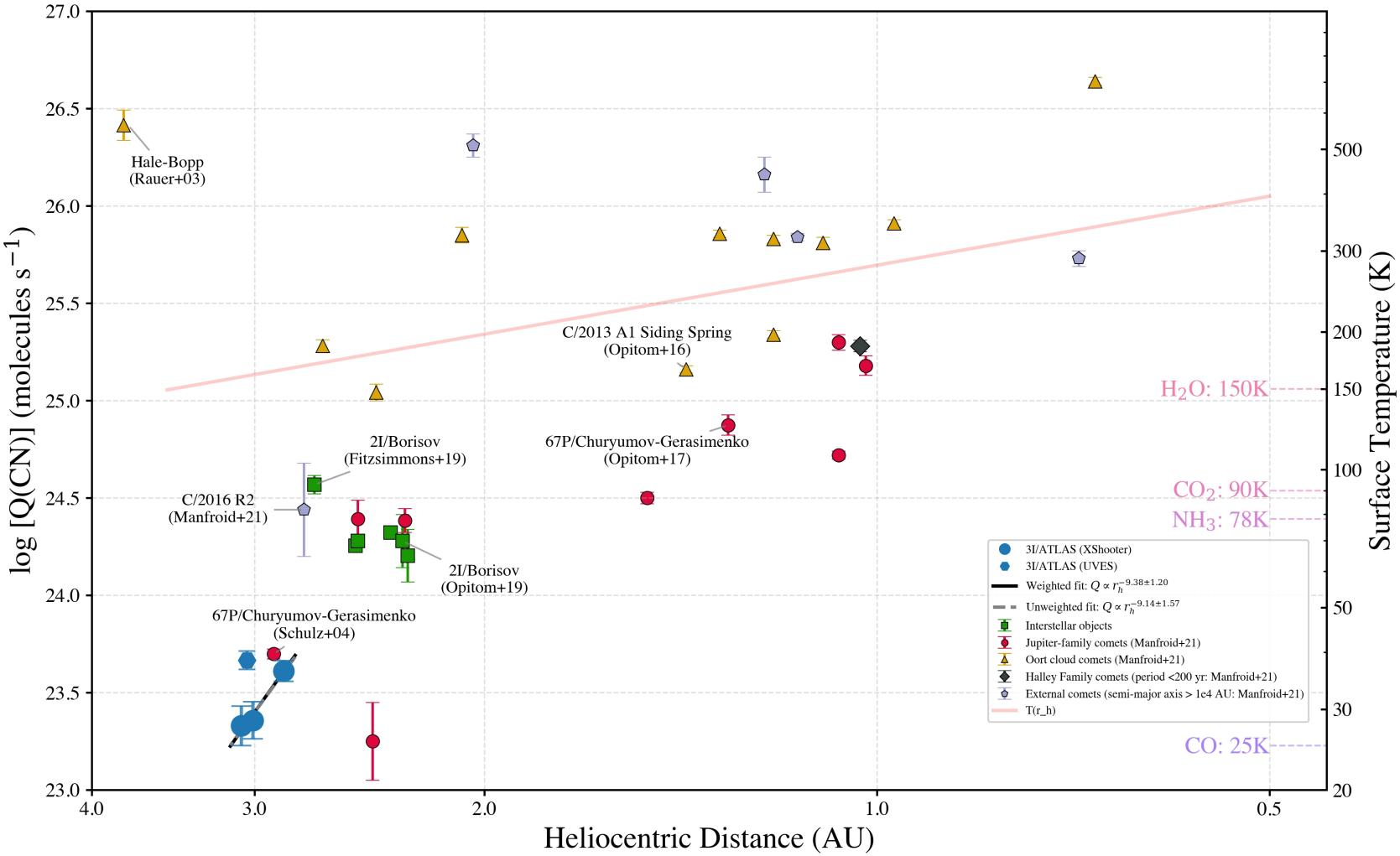

CN production rates – comparison with Solar System comets and 2I/Borisov (Rahatgaonkar et al. 2025).

3I/ATLAS: Ni to Fe ratio

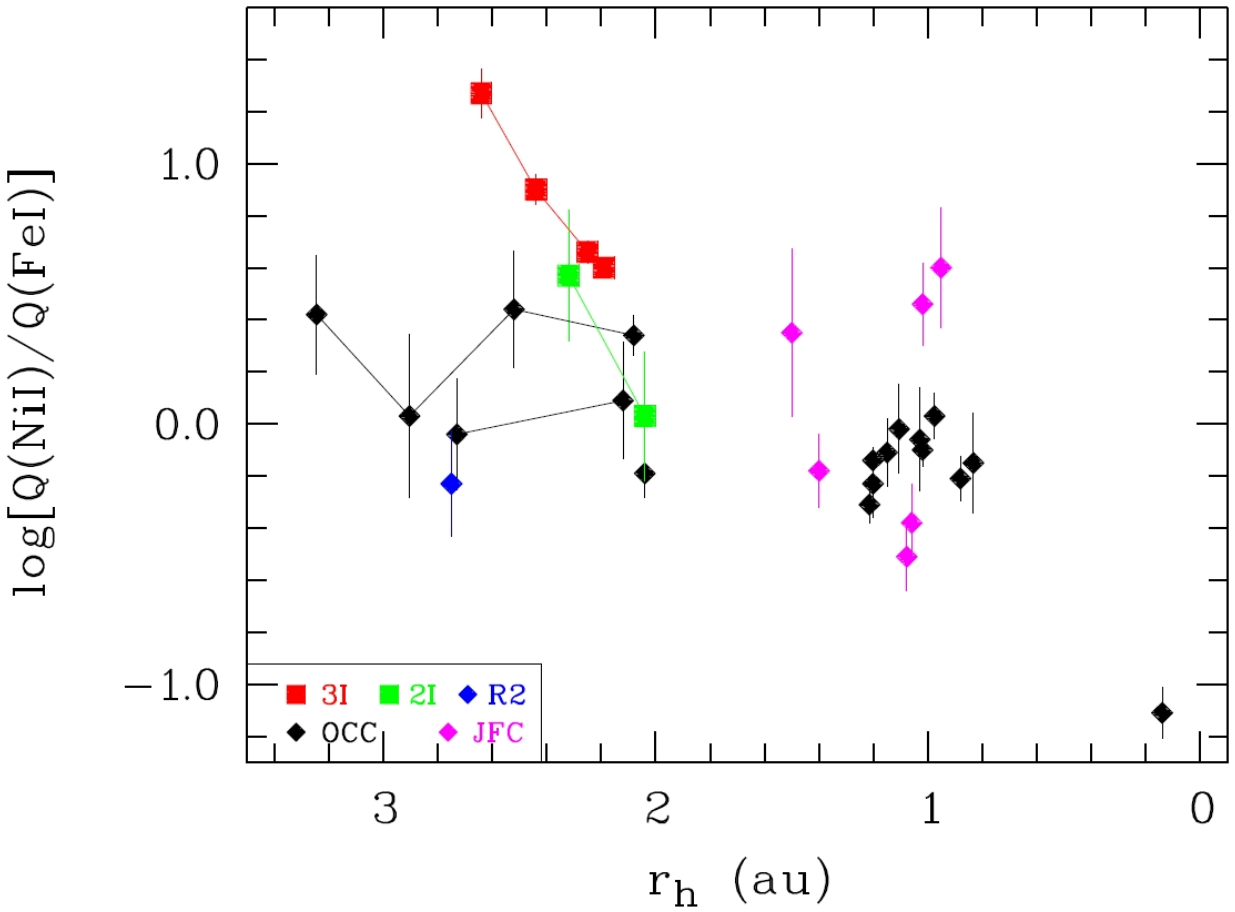

Atomic Ni to Fe production-rate ratio as a function of heliocentric distance (Hutsemékers et al. 2025).

3I/ATLAS: ALMA - CH_3OH

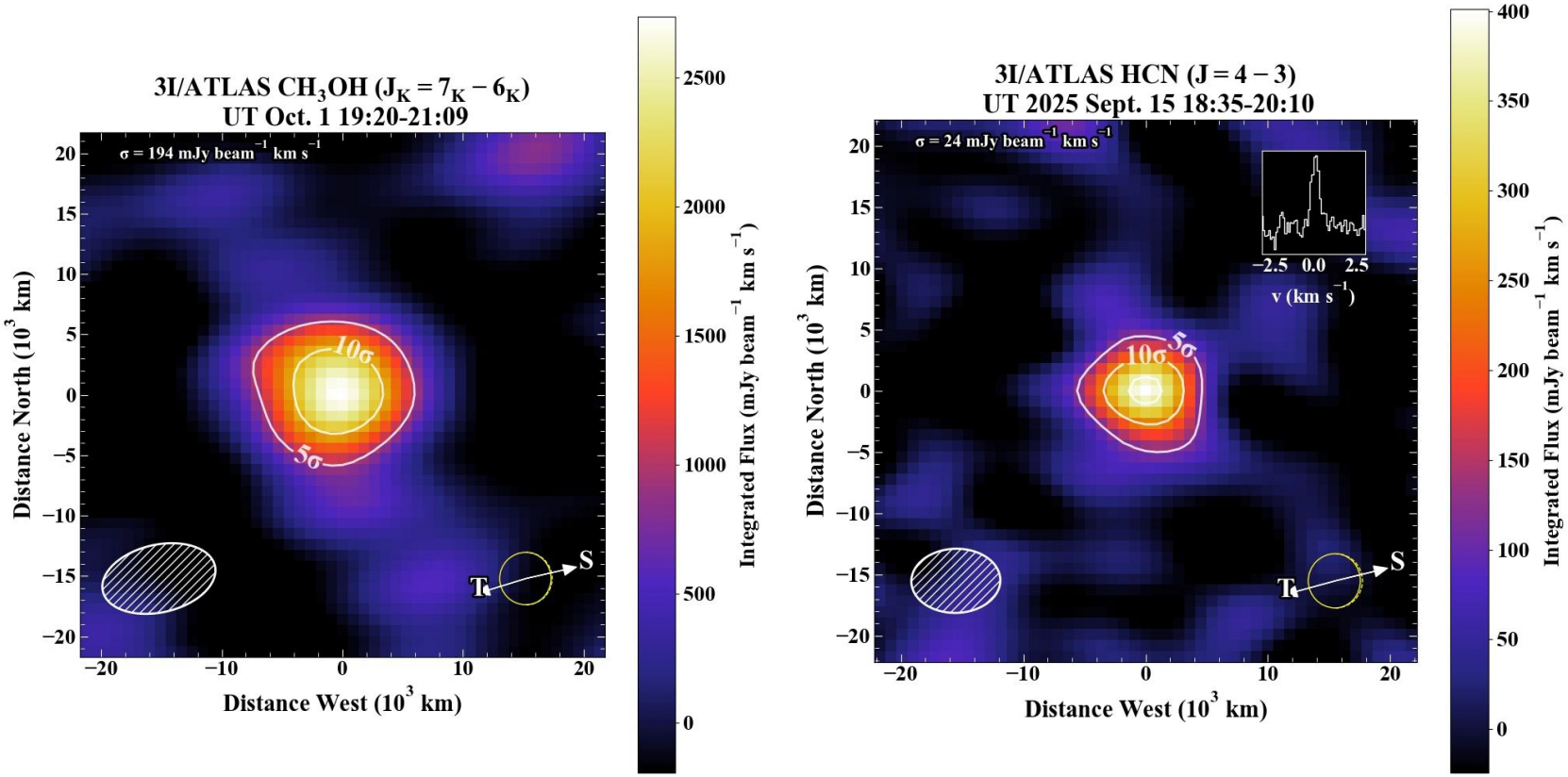

Spectrally integrated CH_3OH and HCN flux maps (Roth et al. 2025).

3I/ATLAS: CH_3OH vs HCN

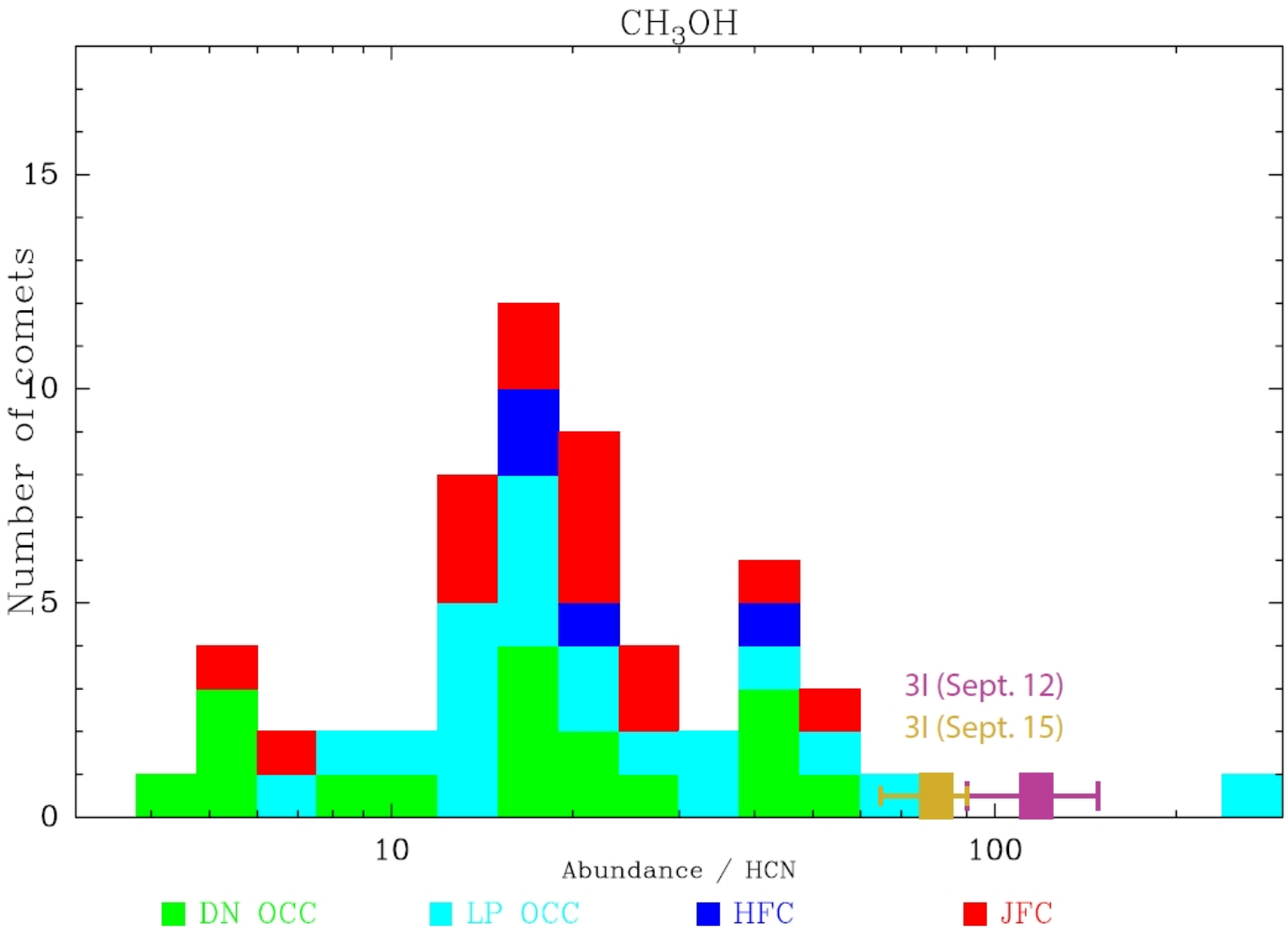

CH_3OH to HCN ratio in Solar System comets and in 3I/ATLAS (Roth et al. 2025).

3I/ATLAS: Potential thermal profiles

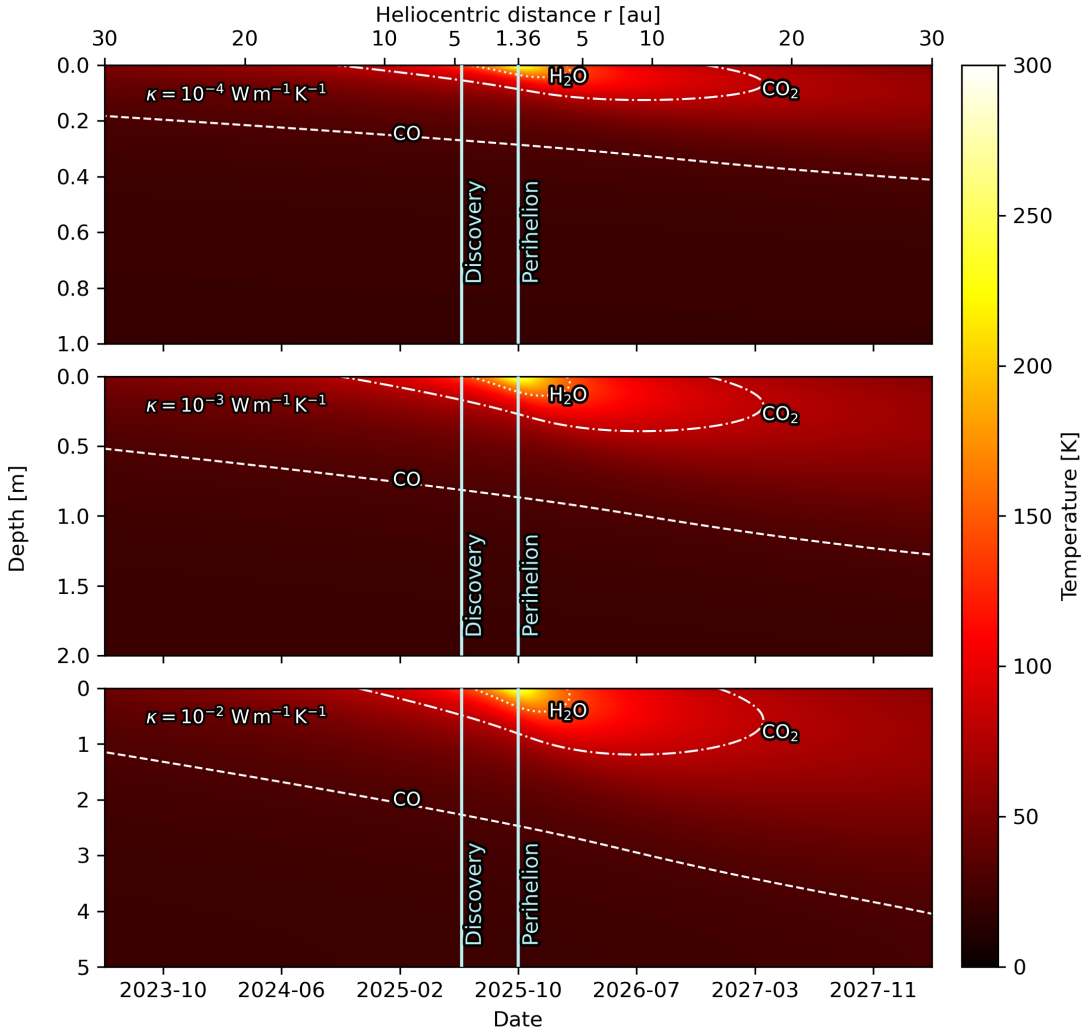

Simulations of thermal profiles of the outer layer of the 3I nucleus (Yaginuma et al. 2025).

3I/ATLAS: observing campaign

- Ground-based: ATLAS, ZTF, NOT, GTC, Gemini, VLT, ...
- Rubin Observatory (LSST): commissioning / validation images.
- Space telescopes: HST, JWST, SPHEREx, Swift.
- Mars missions: MRO, MAVEN, Perseverance, Mars Express, ExoMars TGO.
- Solar/heliospheric: SOHO, STEREO, PUNCH, GOES, ...

3I/ATLAS: MAVEN - hydrogen Lyman-α

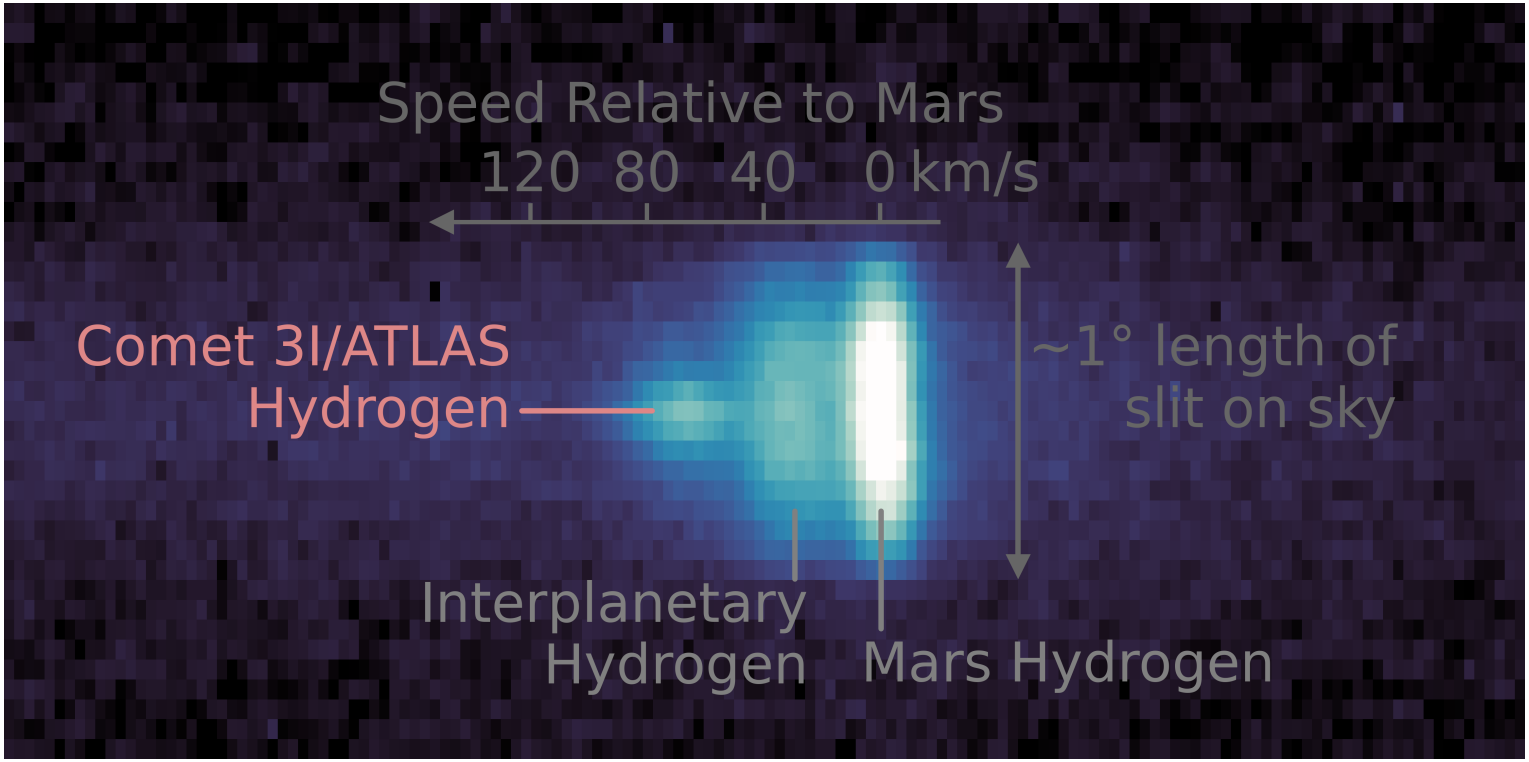

Hydrogen Lyman-α emission as seen by MAVEN (Mars Atmosphere and Volatile Evolution, NASA/Goddard/LASP/CU Boulder).

3I/ATLAS: Solar observatories - lightcurve

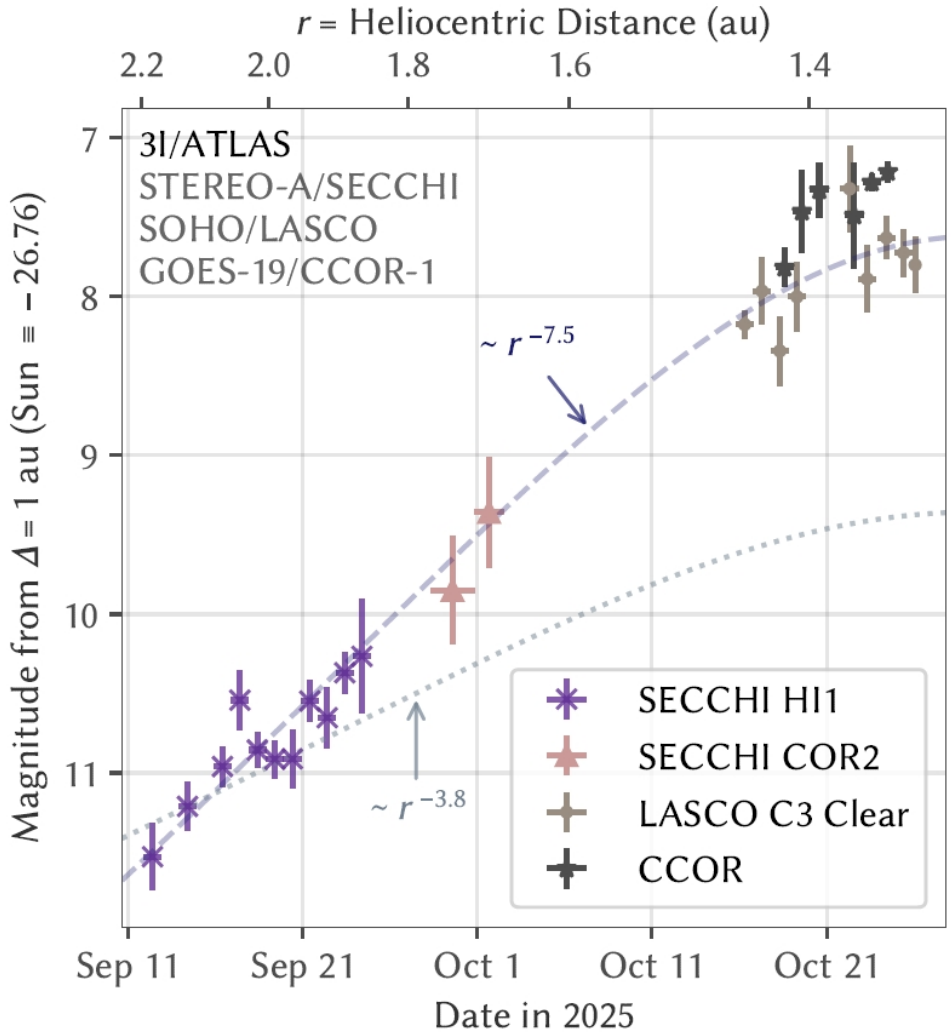

Light curve around solar conjunction, measured from SOHO, STEREO and GOES images (Zhang & Battams 2025).

3I/ATLAS: gas production rates (H_2O, OH, CO_2, CO)

Species	r_H [au]	Q [s^{-1}]	Instrument / ref.
H_2O	4.41	$< 9.1 \times 10^{26}$	VLT/X-shooter (Alvarez-Candal+ 2025)
H_2O	3.51	7.4×10^{26}	Swift/UVOT (Xing+ 2025)
H_2O	3.32	2.2×10^{26}	JWST/NIRSpec, terminal (Cordiner+ 2025)
H_2O	2.90	1.4×10^{27}	Swift/UVOT (Xing+ 2025)
OH	4.41	$< 8.2 \times 10^{26}$	VLT/X-shooter (Alvarez-Candal+ 2025)
OH	3.17	$< 7.8 \times 10^{23}$	VLT/X-shooter (Rahatgaonkar+ 2025)
OH	2.64	2.3×10^{26}	VLT (Hutsemékers+ 2025)
OH	2.45	3.9×10^{26}	VLT (Hutsemékers+ 2025)
OH	2.25	1.1×10^{27}	VLT (Hutsemékers+ 2025)
OH	2.19	1.4×10^{27}	VLT (Hutsemékers+ 2025)
OH	1.76	1.67×10^{28}	TRAPPIST-North (Jehin+ 2025, ATel 17515)
CO_2	3.32	1.7×10^{27}	JWST/NIRSpec, terminal (Cordiner+ 2025)
CO	3.32	3.7×10^{26}	JWST/NIRSpec, terminal (Cordiner+ 2025)

3I/ATLAS: gas production rates (CN, C_2)

Species	r_H [au]	Q [s^{-1}]	Instrument / ref.
CN	4.41	$< 5.6 \times 10^{23}$	VLT/X-shooter (Alvarez-Candal+ 2025)
CN	3.14	1.0×10^{24}	VLT (Hutsemékers+ 2025)
CN	3.07	2.1×10^{23}	VLT/X-shooter (Rahatgaonkar+ 2025)
CN	3.04	4.6×10^{23}	VLT/UVES (Rahatgaonkar+ 2025)
CN	3.04	2.2×10^{24}	VLT (Hutsemékers+ 2025)
CN	3.01	2.3×10^{23}	VLT/X-shooter (Rahatgaonkar+ 2025)
CN	2.91	7.6×10^{24}	Lowell 1.1m (Schleicher 2025, ATel 17352)
CN	2.85	4.1×10^{23}	VLT/X-shooter (Rahatgaonkar+ 2025)
CN	2.64	6.2×10^{24}	VLT (Hutsemékers+ 2025)
CN	2.45	9.1×10^{24}	VLT (Hutsemékers+ 2025)
CN	2.25	7.1×10^{24}	VLT (Hutsemékers+ 2025)
CN	2.22	1.4×10^{25}	VLT (Hutsemékers+ 2025)
CN	2.19	2.0×10^{25}	VLT (Hutsemékers+ 2025)
CN	2.14	1.8×10^{25}	VLT (Hutsemékers+ 2025)
CN	1.76	5.5×10^{25}	TRAPPIST-North (Jehin+ 2025, ATel 17515)
C_2	2.64	4.0×10^{24}	VLT (Hutsemékers+ 2025)
C_2	2.45	4.0×10^{24}	VLT (Hutsemékers+ 2025)
C_2	2.25	2.3×10^{24}	VLT (Hutsemékers+ 2025)
C_2	2.19	3.0×10^{24}	VLT (Hutsemékers+ 2025)
C_2	1.76	6.1×10^{25}	TRAPPIST-North (Jehin+ 2025, ATel 17515)

3I/ATLAS: metal production rates (Ni, Fe)

Species	r_H [au]	Q [s^{-1}]	Instrument / ref.
Fe I	~ 3.1	$< 6.8 \times 10^{21}$	VLT (Hutsemékers+ 2025, 2025-08-12/20)
Fe I	3.04	$< 1.4 \times 10^{22}$	VLT (Hutsemékers+ 2025, 2025-08-15/14)
Fe I	2.64	1.0×10^{22}	VLT (Hutsemékers+ 2025, 2025-08-28)
Fe I	2.45	4.1×10^{22}	VLT (Hutsemékers+ 2025, 2025-09-03/04)
Fe I	2.25	1.2×10^{23}	VLT (Hutsemékers+ 2025, 2025-09-10)
Fe I	2.19	1.6×10^{23}	VLT (Hutsemékers+ 2025, 2025-09-12)
Ni I	3.88	1.8×10^{21}	VLT (Rahatgaonkar+ 2025)
Ni I	3.78	2.8×10^{21}	VLT (Rahatgaonkar+ 2025)
Ni I	3.65	5.9×10^{21}	VLT (Rahatgaonkar+ 2025)
Ni I	3.55	6.6×10^{21}	VLT (Rahatgaonkar+ 2025)
Ni I	3.23	1.1×10^{22}	VLT (Rahatgaonkar+ 2025)
Ni I	3.14	6.0×10^{22}	VLT (Rahatgaonkar+ 2025)
Ni I	~ 3.1	6.6×10^{22}	VLT (Hutsemékers+ 2025, 2025-08-12/20)
Ni I	3.07	1.7×10^{22}	VLT (Rahatgaonkar+ 2025)
Ni I	3.04	5.5×10^{22}	VLT (Hutsemékers+ 2025, 2025-08-15/14)
Ni I	3.04	5.8×10^{22}	VLT (Rahatgaonkar+ 2025)
Ni I	3.01	2.0×10^{22}	VLT (Rahatgaonkar+ 2025)
Ni I	2.85	4.7×10^{22}	VLT (Rahatgaonkar+ 2025)
Ni I	2.64	1.9×10^{23}	VLT (Hutsemékers+ 2025, 2025-08-28)
Ni I	2.45	3.2×10^{23}	VLT (Hutsemékers+ 2025, 2025-09-03/04)
Ni I	2.25	5.6×10^{23}	VLT (Hutsemékers+ 2025, 2025-09-10)
Ni I	2.19	6.3×10^{23}	VLT (Hutsemékers+ 2025, 2025-09-12)

3I/ATLAS: gas production rates – other species

Species	r_H [au]	Q [s^{-1}]	Instrument / ref.
OCS	3.32	1.7×10^{24}	JWST/NIRSpec, terminal (Cordiner+ 2025)
NH	1.76	2.31×10^{25}	TRAPPIST-North (Jehin+ 2025, ATel 17515)
HCN	3.29	$< 0.6 \times 10^{25}$	JCMT, $J = 3$–2 (Coulson+ 2025)
HCN	3.00	$< 1.0 \times 10^{25}$	JCMT, $J = 3$–2 (Coulson+ 2025)
HCN	2.81	$< 1.0 \times 10^{25}$	JCMT, $J = 3$–2 (Coulson+ 2025)
HCN	2.63	$< 1.0 \times 10^{25}$	JCMT, $J = 3$–2 (Coulson+ 2025)
HCN	2.45	$< 1.0 \times 10^{25}$	JCMT, $J = 3$–2 (Coulson+ 2025)
HCN	2.33	1.3×10^{25}	JCMT, $J = 3$–2 (Coulson+ 2025)
HCN	2.17	0.5×10^{25}	ALMA/ACA (Roth+ 2025)
HCN	2.13	4.0×10^{25}	JCMT, $J = 3$–2 (Coulson+ 2025)
HCN	2.08	1.0×10^{25}	ALMA/ACA (Roth+ 2025)
CH_3OH	2.60	5.0×10^{26}	ALMA/ACA (Roth+ 2025)
CH_3OH	2.01	9.6×10^{26}	ALMA/ACA (Roth+ 2025)
CH_3OH	1.90	1.2×10^{27}	ALMA/ACA (Roth+ 2025)
CH_3OH	1.69	2.3×10^{27}	ALMA/ACA (Roth+ 2025)

3I/ATLAS: COBS - lightcurve

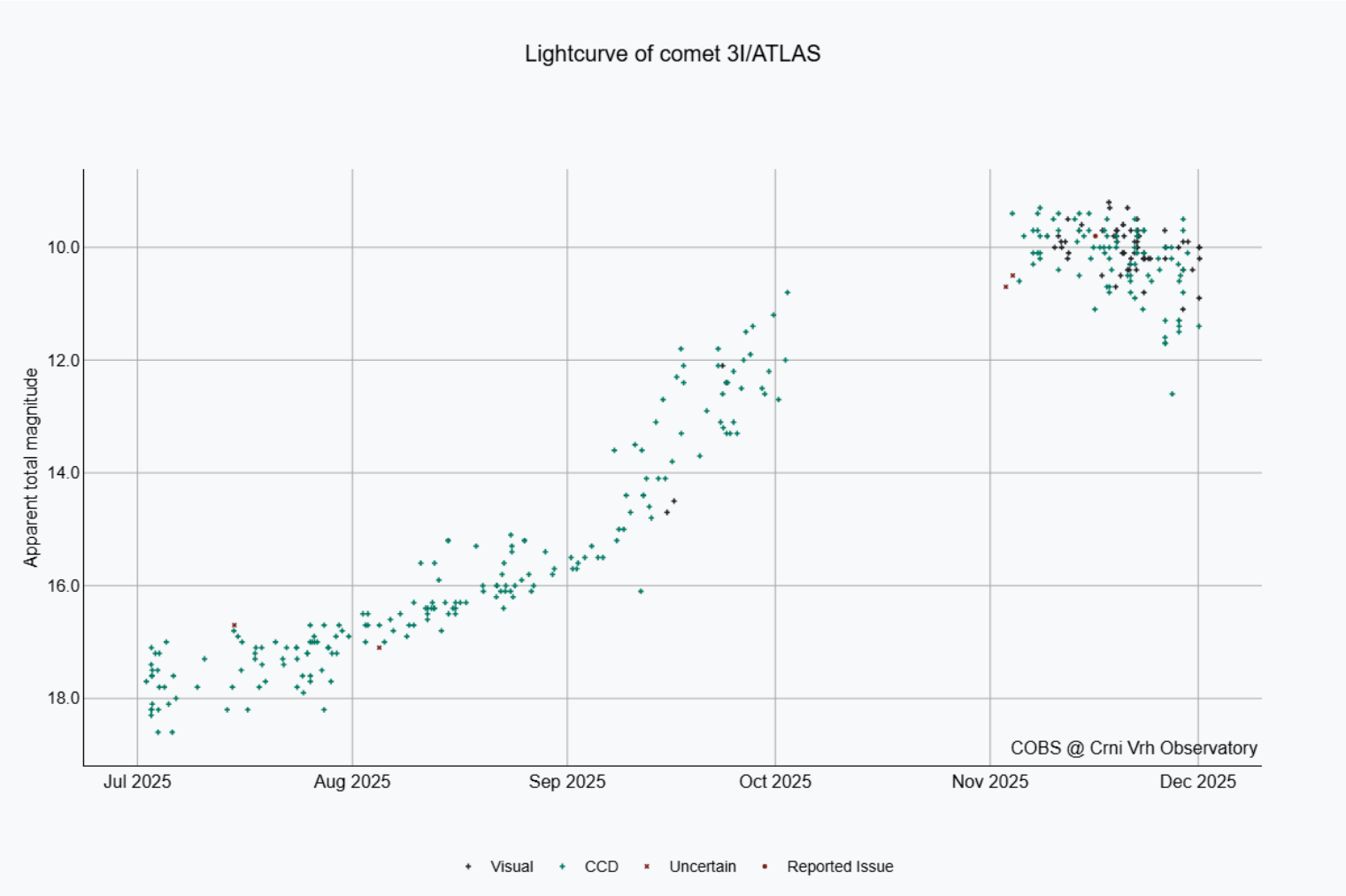

Up-to-date light curve from observations reported to the Comet Observation Database (https://cobs.si/).

3I/ATLAS: amateur image

3I/ATLAS imaged with amateur 25 cm telescope on 19 November 2025 (credit: Mariusz Świętnicki).

Interstellar objects: a bridge to other planetary systems